REACTION CONDITION EFFECTS ON RE(VII) SORPTION KINETICS AT THE ZEROVALENT IRON-WATER INTERFACE

BY

BRIAN LENELL

THESIS

Submitted in partial fulfillment of the requirements
for the degree of Master of Science in Natural Resources and Environmental Sciences
in the Graduate College of the
University of Illinois at Urbana-Champaign, 2016

Urbana, Illinois

Adviser:

Assistant Professor Yuji Arai

Abstract

Long lived technetium-99 (^{99}Tc) ($t_{1/2}$: 2.1 x 10^5 yr) is one of the major radionuclide risk drivers in low level radioactive waste (LLW) at U.S. Department of Energy sites. Cementitious waste technology (CWT)is presently being used to immobilize LLW. Blast furnace slag is presently being added to the CWT formulation to promote reductive precipitation of the dominant risk driver, pertechnetate, $^{99}Tc(VII)O_4^-$ to the sparing soluble $^{99}Tc(IV)$. Some previous studies show that a variety of hazardous elements immobilized by slag can still remain mobile and leach out of the cement systems. Therefore, use of additional reducing agents should be tested. Because LLW is in caustic brine (high nitrate) solutions, it is a challenging task to reduce $^{99}Tc(VII)O_4^-$. This study evaluated the reducing capacity of zero valent iron (ZVI) as a potential reducing agent in the CWT. Using perrhenate ($Re(VII)O_4^-$) as a chemical analogue for $^{99}Tc(VII)O_4^-$, batch Re(VII) sorption experiments were conducted in ZVI as a function of pH (8.2-10.2) and nitrate concentration (0-0.1M). Zero valent iron was effective in reducing Re(VII) to Re(IV), and the initial (< few hrs.) Re sorption was rapid at the ZVI-water interface followed by a slow uptake. Although the extent of Re sorption decreased with increasing pH and nitrate concentration, ZVI immobilized Re(VII) by as much as 10% at pH 10.2. The results suggest that ZVI can be a potential reducing agent to improve the performance of CWT to immobilize $^{99}Tc(VII)O_4^-$.

Acknowledgements

Foremost, I would especially like to thank my advisor Dr. Yuji Arai for all he has done to help me with this project. Without his constant guidance and efforts, this research project would have not been possible. The support he has given me has not only increased my scientific knowledge, but has also helped further sculpt my professionalism. He has always pushed me to do my very best and I owe him my upmost gratitude over the past years for helping me build my own confidence and shape me into the person who I am today.

I also thank my committee members Dr. Richard Mulvaney and Dr. Daniel Kaplan for their feedback and support of my research. Also, thanks to Martin Pentrak and Corey Mitchell for sacrificing their own time and assisting me with additional data collection. Their efforts are greatly appreciated.

Finally I would like to thank my parents, because without their support throughout my life I would not have such amazing and unique opportunities such as this. They created a firm foundation of my character that has allowed me to live up to my full potential.

Table of Contents

Chapter 1: Introduction and Literature Review

1.1 Geologic Occurrence and Productions of Technetium

Radioactive Tc isotopes are of both natural and anthropogenic origin. But anthropogenic ^{99}Tc sources far outweigh natural sources. They are nuclear power plants, global weapons, and nuclear accidents in Chernobyl, Russia and Fukushima, Japan (Icenhower et al., 2010; Momoshima et al., 1995; Momoshima et al., 2005; Shi et al., 2012; Vandergraaf et al., 1984). While all Tc isotopes (e.g., ^{97}Tc, ^{98}Tc, ^{99}Tc) are unstable, only ^{99}Tc is of the major concern in our environment because of its presence and a long half-life (2.1×10^5 yr).

In nature, ^{99}Tc results from the spontaneous fission of ^{238}U, neutron induced fission of ^{235}U, or cosmic ray reactions with molybdenum, ruthenium and niobium within the earth's crust (Shi et al., 2012). These various formations may have produced about 60 pBq of Tc, but a negligible amount at the earth's surface. Several millenniums ago, the Oklo natural nuclear reactors in Gabon, Africa, served as a point source for ^{99}Tc. These self-sustaining fission reactors may have produced 730 kg Tc, which has now nearly completely decayed to ^{99}Ru (Gauthier-Lafaye et al., 1996; Icenhower et al., 2010; Yoshihara, 1996).

Levels of ^{99}Tc released into the environment from nuclear weapons testing are between 100 and 160 TBq (Schulte and Scoppa, 1987; Yoshihara, 1996). The formation of Tc during testing and detonation of nuclear weapons is primarily by fission of ^{235}U or ^{239}Pu. Most testing occurred in the northern hemisphere starting in the 1950's. Well known underground nuclear tests at Nevada weapons testing sites in North America have released ~ 21 TBq of ^{99}Tc (Shi et al., 2012). However, this testing was banned in 1963, with concentration levels of ^{99}Tc in rainwater showing a continual decrease afterwards.

Common nuclear reactors under normal operating conditions can produce around 1 MBq per year (Schwochau, 2000). Studies measuring ^{99}Tc release rates from pressurized water reactors show a flux of 8.1×10^2 Bq/yr (Luykx, 1986). Other values reported are between 400 and 500 GBq/MT of fuel spent from a reactor (Icenhower et al., 2010). One of the greatest anthropogenic sources of ^{99}Tc is from nuclear reprocessing facilities, where nuclear fuel rods are sent for disposal. Technetium-99 is removed from the fuel rods. The release of ^{99}Tc into the environment up to 1986 is estimated to be ~1000 TBq (equivalent to 1600 kg) (Tagami, 2003).

1.2 Toxicity of Technetium

Technetium (Tc) is a radioactive element formed during induced fission of ^{235}U in nuclear reactors, and also nuclear bombs. Technetium-99 is a common long lived radioactive isotope formed during these processes, having a half-life of 2.13×10^5 years. The type of radiation emitted by Tc-99 is β^- emissions and the specific activity of ^{99}Tc is 629 kBq/mg (Schwochau, 2000). From nuclear fuel sources, ^{99}Tc is often introduced into the aquatic and terrestrial environment as soluble pertechnetate (TcO_4^-) ions. Therefore, humans are potentially exposed to ^{99}Tc via consumption of contaminated water and food, accumulating ^{99}Tc in the thyroid and gastrointestinal tract. Inhalation of volatile ^{99}Tc compounds could damage lung tissues (Van Bruwaene et al., 1986). The EPA has established that the contamination level of radionuclides that are β- particle or photon emitters may have a maximum level of 4 mrem yr^{-1} or 33 Bq/L in drinking water (Icenhower et al., 2010). In excess of this level, ^{99}Tc is known to cause lung cancer or other sickness (e.g., thyroid cancer), and is more concerning than the current level of typical ^{99}Tc ingestion through water or food (Radioisotope Safety, 2013; Van Bruwaene et al., 1986).

1.3 Stabilization and Solidification Technology

In order to reduce the risk of radiation release to environment, many remediation and immobilization technologies have been considered. Some methods include macroencapsulation and containerization, soil vapor extraction, and thermal treatment. Other ex-situ methods include incineration, vitrification, chemical extraction, excavation, and solidification/stabilization (USEPA, 2007). Of all technologies, solidification and stabilization (S/S) technology using cementitious materials has been one of the major focuses of U.S. Department of Energy to treat radionuclides like ^{99}Tc (Peters, 1999).

Ordinary Portland cement (OPC) is commonly used in the S/S technology. Although the formulations are varied depending on the waste forms and the type of contaminants (Navarro-Blasco et al., 2013; Querol et al., 2006; Wiles, 1987), the major chemical composition of OPC is silicate, aluminum oxide and calcium oxide (Gilliam et al., 1990; Harbour et al., 2006) (Table B.1). The CaO content is known to provide a superior buffer capacity to maintain alkaline pH ~12 (Angus and Glasser, 1985; Atkins and Glasser, 1992).

The cement setting process of OPC is facilitated by the hydration of alite (Ca_3SiO_5) and belite (Ca_2SiO_4). The majority of the hydration process occurs in <30 days (Glasser, 1997; Paria and Yuet, 2006). The hydration of alite results in a calcium silicate hydrate gel. The hardened product of OPC can have a range of different pore sizes. It is possible for contaminants to leach out, which can compromise its effectiveness. Based on the immobilization/stabilization treatment of contaminants, S/S technology is categorized into three types. They are physical, chemical and thermal S/S technologies (Conner and Hoeffner, 1998).

Solidification of OPC could physically encapsulate wastes in fine or individual waste particles (microencapsulation) or large containers of waste (macroencapsulation) (Malviya and Chaudhary, 2006; Mulligan et al., 2001). However the encapsulation technique alone does not provide the long term stability of contaminants in the cementitious waste form (CWF). Refining cement S/S technology, chemical and/or thermal conversion of contaminants into less soluble and/or toxic forms is more desirable to reduce the hazard potential to the environment (Conner and Hoeffner, 1998; Glasser, 1997; Yousuf et al., 1995).

1.4 Mechanisms of chemical immobilization in S/S technology

While the thermal conversion of contaminants in the S/S technology remains important, the chemical immobilization of ^{99}Tc(VII) is the major focus of U.S. DOE S/S technology. The chemical immobilization is accomplished by the combination of precipitation, adsorption or redox reaction (Paria and Yuet, 2006). These mechanisms are due to interaction between the contaminant species and the hydration products of cement. A few examples of each mechanism are summarized below.

Precipitation reaction

There are two different precipitation mechanisms in the S/S technology, precipitation of metal carbonates/oxides and co-precipitation of metals within PC reaction products (Chen et al., 2009; Pollard et al., 1991; Zhou and Haynes, 2010).

Ordinary Portland cement was used in an experiment to immobilize metals like lead (Walton et al., 1997). A major trend discovered in the study is that pH is a major factor in the leachability of Pb in the cement blocks. More basic pH values showed that Pb leaching was reduced with increasing pH and curing time (Gollmann et al., 2010). Raising the pH value of the

contamination area is also important because it causes the dissolved metals to precipitate as hydroxides or carbonates (Yeung, 2010). The solubility of most metals is significantly reduced with increasing pH from 7 to 11(Conner and Hoeffner, 1998). This formulation of Ca/Mg-phosphate aluminum systems induces a higher pH than the pure OPC system, resulting in the formation of insoluble hydroxides such as $Pb(OH)_2$ and CuO (Buj et al., 2010; Fernandez et al., 2014). Metal hydroxides have a different solubility depending on their species and the pH of the solution they interact with. The reaction products may vary among different metals. This is because the metals react much differently with the S/S reagent/components depending on environment and contaminant variety. However, it should be noted that metals can potentially change their speciation during aging (Conner and Hoeffner, 1998), resulting in changes in solubility.

Various additives (e.g., Al_2O_3, fly ash, lime, elemental sulfur, ferrous sulfate, phosphates, gypsum) can be added to OPC to enhance the immobilization of metals and metalloids (Mallampati et al., 2013; Navarro-Blasco et al., 2013; Querol et al., 2006). Elemental sulfur can be used in an alkaline system. The reaction of S(0) and hydroxyl ions forms polysulfide ions, which then react with the metals (Conner and Hoeffner, 1998). The formation of metal polysulfide co-precipitates is one of desirable low solubility precipitates to immobilize metals.

The addition of fly ash or lime is known to induce the precipitation of calcium-arsenic complex (Ca-As) (Bothe and Brown, 1999; Moon et al., 2004; Singh and Pant, 2006). Arsenic is also immobilized with iron salts, specifically ferrous sulfate ($FeSO_4$) (Kumpiene et al., 2008). Using phosphate-based additives, lead mobility is reduced by precipitation of 'pyromorphite-type' minerals, $Pb_5(PO_4)_3$(F,Cl,Br, or OH) (Miretzky and Fernandez-Cirelli, 2008). These minerals have a low solubility and are not easily mobilized by organisms in soils. The effectiveness of this immobilization technique is dependent on the solubility of reaction products that is influenced by P additive compounds. Therefore, using phosphate-based salts would be most effective because they are more soluble than phosphate rocks (Brown et al., 2004). Selenium is shown to be immobilized by precipitating as selenite (SeO_3^{2-}), a variety of gypsum and selenate (SeO_4^{2-}), which is analogous to sulphate (Moon et al., 2009). The problem with immobilizing Se is that it has a minimum solubility range between pH of 6.5 and 7.5. This range does not fall under the same range as most other metals requiring immobilization.

Changing the valence state of a metal can affect its solubility. For example Cr(VI) can be reduced to Cr(III) using reducing agents such as ferrous, bisulfite, and hydrosulfite. Formulations of cement incorporating blast furnace slag (BFS), containing these reductants, have been used to immobilize Cr. Reduced Cr can readily precipitate out as less soluble $Cr(III)(OH)_3$. Blast furnace slag is a byproduct of iron slag from steel making after being quenched in water to form a glassy material. This material can be incorporated into cement formulations. Kindness et al., (1994) immobilized Cr using Ordinary Portland Cement (OPC) blended with BFS. The results from the experiment showed that Cr was effectively immobilized. This is because slag contain reduced sulfur species such as $S_2O_3^{2-}$, which is able to reduce Cr(VI) to Cr(III).

Alternatives to Portland cement have been studied to immobilize wastes. Zhou et al., (2006) used a calcium sulfoaluminate cement (CAS) to act as the primary material to immobilize inorganic contaminants like As and Pb. The main hydration phase in this cement system is called ettringite, which is a prismatic mineral that can also form needles. It has a molecular formula of $Ca_6Al_2(SO_4)(OH)_{12}\cdot 26(H_2O)$. This mineral has capacity to incorporate metals within the structure, resulting in the co-precipitation of metals.

Alkali-activated slag (AAS) mixtures have been used to immobilize Hg and Zn. Mercury ions were immobilized by chemical fixation within the cement matrix. These mixtures include BFS as one of its primary ingredients. The C-S-H hydration product of the AAS causes the formation of metal silicate co-precipitates and formation of HgO and insoluble zinc silicate gel (Qian et al., 2003a; Qian et al., 2003b).

Adsorption reaction

Adsorption could also play an important role in metal immobilization. Adsorption of metal cations greatly depends on the adsorptive and adsorbate characteristics, such as electron affinity, surface area, and surface charge density (Zhou and Haynes, 2010).

Adsorption of metal contaminants onto cement grains and additives (e.g., clays) is a common mechanism of immobilization. Adsorption reactions are often reversible, pH-dependent, and specific to the targeted contaminant and sorbent. For this reason, the requirement of specific chemical conditions is the key for long-term storage. Generally, adsorption of heavy metals on cement components increases with increasing pH (Cocke, 1990; Hsi and Langmuir, 1985; Moon and Dermatas, 2006; Yeung, 2010). Experiments using BFS as an additive in cement

formulations show a higher adsorption with lead (Srivastava et al., 1997). It is believed that this occurs because of an increasing negative charge density on the slag surfaces at high pH.

Clay minerals (e.g., kaolinite, smectite) and synthetic minerals (e.g., alumina and zeolite) have also been used as additives in cement mixtures. Montmorillonite and kaolinite have been frequently incorporated into the cement mixture to immobilize heavy metals (Moon and Dermatas, 2006). The use of montmorillonite is more effective in reducing the leaching of Pb than kaolinite due to its higher cation exchange capacity. Another study used a mixture of Class C fly ash and kaolinite to immobilize Ni and Zn (Tomasevic et al., 2013). The fly ash and kaolinite combination showed a decrease in leachability of these metals. The use of synthetic zeolite and hydrated alumino-silicates is another example. Zeolites are primarily used to treat inorganic contaminants to increase the surface site to facilitate the adsorption of metals (Querol et al., 2006; Yeung, 2010). Alumina can be added to calcium aluminate cement (CAC) (i.e., Al_2O_3 content is at least 30 to 35% by weight) to maximize its immobilization potential for metals (Hidalgo et al., 2007). Other minerals such as hydrogarnet ($Ca_3Al_2(SiO_4)_{3-x}(OH)_{2x}$ and gehlenite $Ca_2Al_2SiO_7{\cdot}8H_2O$ have been also used to increase the retention of heavy metals in CAC.

Aside from the mineral additives, cement hydration products such as calcium silicate hydrate gel (C-S-H) and a calcium aluminate hydrate gel (C-A-H) are also known to increase the retention of heavy metals (Chen et al., 2009; Hong and Glasser, 2002; Li et al., 2001). The newly formed amorphous solid acts as a sink to effectively retain cations. The hydration reaction of calcium aluminate hydrate gel is shown below.

$C_3S + H_2O \rightarrow Ca^{2+} + OH^- + H_4SiO_4 \rightarrow C—S—H + Ca(OH)_2$ (Chen et al., 2009)

Pores in the gel give a higher surface area to the grains and increase the capacity for binding with metal cations (Hong and Glasser, 2002). The enhanced adsorption of metals in the C-S-H gels has been supported by the several surface complexation models, double electrostatic layer model (bi-layer model), triple layer model (Yousuf et al., 1995), and the charge dispersal model (Chen et al., 2007).

Redox reaction

As discussed by Conner and Hoeffner (1998), another important immobilization mechanism for redox sensitive metal(loid) is the alternation of its redox potential. Changing the oxidation state of these contaminants could facilitate adsorption and/or precipitation processes. Having strong oxidants or reductants in a system can greatly influence the valence state of metals. In the adsorption section, the reductive precipitation of Cr(VI) was discussed with the addition of slag. After the hydration process of these cement mixtures, reduced sulfur species facilitate the reduction of Cr(VI) to Cr(III) (Deja, 2002). In the case of arsenic(As), mobile arsenite, As(III), can be oxidized to arsenate, As(V). The change in As speciation increases the sorption capacity of As in minerals. In general, As(V) is more reactive in geomedia than As(III) (Arai et al., 2001).

The chemical stabilization of radioactive element, ^{99}Tc, is also facilitated by the reduction of Tc(VII) to Tc(IV) (Langton, 1987). Pertechnetate exists at E_h values at or below 0.220 V and neutral pH conditions. Since Tc(VII) anions are non-reactive with mineral surfaces, immobilization of Tc requires the reduction of Tc(VII) to Tc(IV). Once reduced, Tc(IV) readily form (oxy)hydroxides and or sulfides, resulting in immobilization of Tc (Mattigod et al., 2009). In the current S/S technology at the Savannah River DOE site, slag/grout has been added to Portland Cement (PC) fly ash. Ferrous and sulfide in slag contribute to maintain the reduced redox conditions, Eh: ~80 mV to -300mV, resulting in the Tc reduction (Angus and Glasser, 1985; Atkins and Glasser, 1992; Gilliam et al., 1990).

1.5 Current cementitious waste form technologies for ^{99}Tc immobilization

The nuclear processing plants in the United States, the Savannah River Site (SRS) in South Carolina and the Hanford Site (HS) in Washington, house 80 million gallons of high-level waste (HLW) from the cold war (Lukens et al., 2007). This waste is separated into a high-activity stream, which has high levels of radioactivity at a low volume, and the low-activity waste stream with opposite proportions. At the HS and the SRS, S/S technology has been used to treat ^{99}Tc in the low level waste (LLW).

At the SRS, the total amount of radioactivity for all isotopes stored at this facility is around 1.58×10^{19} Bq (USNRC, 2005). At this facility, the DOE intends to stabilize and dispose of the waste contained in all of their treatment tanks. Disposal strategies for ^{99}Tc at this facility

involve incorporating a salt solution containing low-level radioactive waste with a dry mixture of chemical binders containing cement, blast furnace slag (BFS), and fly ash to form a grout mixture (USNRC, 2005). The weight percentages of these dry ingredients are 10% cement, 45% fly ash, and 45% BFS. Blast furnace slag is used in treatment formulas in order to facilitate a reducing environment to immobilize redox-sensitive elements, such as ^{99}Tc (Cantrell and Williams, 2013). Research has been done to examine the sorption of ^{99}Tc in saltstone mixtures containing 45% BFS and 95% BFS. These mixtures had K_d values of 1000 mL/g and 10,000 mL/g respectively, at a pH of 11.6. Reduction capacity of the standard 45% BFS saltstone blend provides a reduction capacity of 820 µeq/g (Kaplan et al., 2011). Cantrell and Williams (2013) also state that further reduction of Tc can occur over time when encased in saltstone. A major concern is to limit the saltstone oxygen exposure. Oxidation is commonly the mechanism for ^{99}Tc release from the saltstone. Careful observation of these parameters help ensure that ^{99}Tc remains in the stable oxidation state of Tc(IV) for when it is sent to the disposal area. After the waste has been stabilized using the saltstone technology, it will be isolated in an engineered containment vault called the Saltstone Disposal Facility (SDF). The SDF is first filled with the saltstone mixture with stabilized isotopes, and then a clean grout layer is poured between the saltstone and the roof. The vault has a final enclosure of a thick multi-layer cap, and a drainage system. The drainage system diverts the flow of surface water to increase the security of the vault.

The Hanford site also has a waste treatment and immobilization facility operated by the DOE, and is located in southeastern Washington. The fate of the LLW and the secondary liquid waste generated while treating the high level and low level waste is presently slated to be immobilize by vitrification. However, more recently, alternative immobilization approaches are being evaluated, including the use of reducing cementitious waste forms, which is referred to as cast stone. The cast stone blend is near identical to that of SRS's salstone, it includes a mixture of 45% Class F fly ash, 47% Grade 100 BFS, and 8% Type I and II Portland cement (Sundaram et al., 2011). A large inventory of radioactive waste is contained in 177 underground protected tanks, where ^{99}Tc constitutes the long-term disposal major risk driver (Cs-137 accounts by far for the most radioactivity in the take waste). Research done on cast stone immobilization shows that it meets waste requirements set by the Nuclear Regulatory Commission (Pierce et al., 2010). The cast stone blend is similar to saltstone, in that it relies on the reductive capacity of the BFS

additive in order to reduce Tc to less mobile oxidation states. In a leachate analysis of cast stone, the reduced species of Tc was determined as $TcO_2 \cdot nH_2O$ and Tc_2S_7, which is the same species as found in saltstone. Reduction of Tc is highly dependent on the curing time for cast stone, where there is higher reduction for longer curing times. The BFS blend used in cast stone has a reported reductive capacity of 799μeq/g which is slightly lower than in the BFS blend used for saltstone (Um et al., 2015).

1.6 Research Justification

Long-lived radioactive element ^{99}Tc is of particular concern with regard to long-term storage in S/S technologies, because of its calculated high level of risk stemming from its high inventory, long half-life, difficulty in immobilizing in waste forms, and high mobility in the environment. At the US DOE sites (e.g., Savannah River Site and Hanford site), the S/S technology has been used to immobilize ^{99}Tc from low-level liquid waste materials. Due to its high mobility and solubility in subsurface environment, understanding the effective way to reduce $Tc(VII)O_4^-$ in the reducing-CWFtechnology is critical in immobilizing ^{99}Tc. The successful immobilization of Tc in CWF technology depends on the stabilization of Tc and the long term resiliency of CWFs. Consequently, the reducing condition within CWFs is imperative for effective containment.

While the risk of re-oxidation of Tc in CWFs (i.e., effect of oxygen diffusion on the Tc redox chemistry) has been assessed by several researchers (Kaplan, 2003; Lukens et al., 2007; Smith and Walton, 1992), the current cement formulation has not been re-evaluated to improve the reduction capacity of CWFs. Both ferrous (Fe(II)) and sulfur (S(0), S^{2-}) species within slag were thought as important electron donors to reduce Tc(VII) to Tc(IV), resulting in the formation of Tc(IV)-sulfur and or -hydrous oxide species (Allen et al., 1997; Angus and Glasser, 1985). However, there were several reports that these electron donors might not be effective reductants in CWFs. Sulfide in slag is known to rapidly oxidize to sulfate in $Ca(OH)_2$ and Na(OH) alkaline solutions (Roy, 2009). This suggests that sulfides in slag might not serve as the electron donors for Tc(VII) in an alkaline LLW. Ferrous ion is a well-known electron donor serving an important role in redox cycles in CWFs. However, lack of reducing power of ferrous ions for chromate in aqueous and solid phases (e.g., magnetite) has been previously documented in several studies (He et al., 2004; He and Traina, 2005).

While the current formulation (e.g., a mixture of Class F fly ash, Grade 100 or 120 blast furnace slag (BFS), and Type I and II Portland cement) has been tested at HS and SRS, the development of new formulation with stronger reductants will assure the long term stability of CWFs. The discovery of effective reducing agents in CWFs should give insight into the development of new cement formulations. In recent studies, the reduction ability of zerovalent iron has been tested using perrhenate, Re(VII) (Ding et al., 2013). Rhenium is often used as an analogue for Tc because 1) it has a similar Tc oxyanion chemistry (e.g., solubility products) (Wharton et al., 2000) and 2) it is safer to work with due to its non-radioactive characteristics.

Zerovalent iron (ZVI) nanoparticles have been recently used in several studies to reduce ReO_4^- to ReO_2 (Ding et al., 2013). These equilibrium-based geochemical experiments showed the importance of surface area and pH. The removal of Re(VII) occurred much faster using synthetic ZVI (specific surface area: 9.5 m^2/g) than Fe(0) powder (specific surface area: 5.06 m^2/g) at 20ºC and pH 7.0. The pH of the system also influences the perrhenate reduction as well. Liu et al., (2013) tested reductive removal of perrhenate at pH levels of 5.0, 7.0, 8.0, and 10.0. The highest amount of perrhenate reduction occurred at a pH of 8.0 (~98% perrhenate reduced). At high pH levels, it was expected that precipitation of Fe(III) hydroxide would occur on the surface of ZVI particles, prohibiting further electron transfer.

The redox reactions between ZVI and Re(VII) or Tc(VII) are summarized in the theoretical calculation of Gibbs free energy values below. To simulate the alkaline pH LLW form, the following thermodynamic calculations are performed at both standard state and at alkaline pH.

ΔG calculations for reduction of Re and Tc at:

$\Delta G° = -nF\Delta E°$ Where: n = number of e^- per 1 mole reaction

F = Faraday constant

ΔE° = Electrode potential of reaction

<u>Standard State</u>

Re(VII) → Re(IV) reduction by Zero Valent Iron

$$ReO_4^- + 4H^+ + Fe(0) \rightarrow ReO_2 + 2H_2O + Fe(III)$$

$ReO_4^- + 4H^+ + 3e^- \rightarrow ReO_2 + 2H_2O$ $E^0 = 0.51\ V$ (Bard et al., 1985)

$Fe(0) \rightarrow Fe(III) + 3e^-$ $E^0 = 0.04\ V$ (Ebbing and Wrighton, 1993)

$\Delta E = E°_{cathode} - E°_{anode} = (0.51) - (0.04) = 0.47$

$\Delta G° = -3 * 96485.3365 * 0.47 = \mathbf{-136.044\ kJ/mol}$

Tc(VII) →Tc(IV) reduction by Zero Valent Iron

$$TcO_4^- + 4H^+ + Fe(0) \rightarrow TcO_2 + 2H_2O + Fe(III)$$

$TcO_4^- + 4H^+ + 3e^- \rightarrow TcO_2 + 2H_2O$	$E^0 = 0.728$ V	(Cui and Eriksen, 1996)
$Fe(0) \rightarrow Fe(III) + 3e^-$	$E^0 = 0.04$ V	(Ebbing and Wrighton, 1993)

$\Delta E° = E°_{cathode} - E°_{anode} = (0.728) - (0.04) = 0.688$

$\Delta G° = -3 * 96485.3365 * 0.688 = \mathbf{-199.146\ kJ/mol}$

<u>In basic solution</u>

Re(VII) → Re(IV) reduction by Zero Valent Iron

$$ReO_4^- + 2H_2O + Fe(0) \rightarrow ReO_2 + 4OH^- + Fe(III)$$

$ReO_4^- + 2H_2O + 3e^- \rightarrow ReO_2 + 4OH^-$	$E^0 = -0.594$ V	(Bard et al., 1985)
$Fe(0) \rightarrow Fe(III) + 3e^-$	$E^0 = 0.04$ V	(Ebbing and Wrighton, 1993)

$\Delta E = E_{cathode} - E_{anode} = (-0.594) - (0.04) = -0.634$

$\Delta G = -3 * 96485.3365 * -0.634 = \mathbf{183.515\ kJ/mol}$

Tc(VII) →Tc(IV) reduction by Zero Valent Iron

$$TcO_4^- + 2H_2O + Fe(0) \rightarrow TcO_2 + 4OH^- + Fe(III)$$

$TcO_4^- + 2H_2O + 3e^- \rightarrow TcO_2 + 4OH^-$	$E^0 = -0.322$ V	(Cobble et al., 1953)
$Fe(0) \rightarrow Fe(III) + 3e^-$	$E^0 = 0.04$ V	(Ebbing and Wrighton, 1993)

$\Delta E = E_{cathode} - E_{anode} = (-0.322) - (0.04) = -0.362$

$\Delta G = -3 * 96485.3365 * -0.362 = \mathbf{104.783\ kJ/mol}$

In summary, the reduction of TcO_4^- is more thermodynamically favorable compared to the reduction of ReO_4^-. In other words, it could be assumed that if Re was reduced under certain conditions, Tc should be reduced under the same conditions.

While the research evidence and the thermodynamic calculations suggest that ZVI could become a promising additive to the current saltstone/cast stone formulation, one must assume such reactions only occur under the steady-state condition in water (i.e., ionic strength < 0.001 M $NaNO_3$) (Ding et al., 2013; Liu et al., 2013). In order to introduce ZVI to the current ^{99}Tc S/S technology, one must address the knowledge gap between the theoretical reduction capacity of

ZVI and the reduction capacity of ZVI that is specific to complex cement pore water chemistry resulting from the mixing cementitious ingredients with the highly complex and concentrated low level waste aqueous phase. Cement pore water is composed of >50mM of carbonate, sulfate, nitrate at pH >10. Furthermore, the chemical composition of artificial LLW simulant solution is 0.11M $Al(NO_3)_3$, 1.55M NaOH, 0.05M Na_2SO_4, 0.14M Na_2CO_3, 2.11M $NaNO_3$, and 0.33M $NaNO_2$ (Almond et al., 2012).

1.7 Research Objective

The goal of this proposed study is to evaluate the reduction capability of ZVI for perrhenate, as a chemical analogue of pertechnetate, in high carbonate and nitrate solutions. Given the overall goal, the following objectives are set:

1) to develop an appropriate UV-vis Re(VII) spectrophotometric method to speciate Re(VII) in high carbonate and nitrate solutions.

2) to investigate the effect of carbonate and nitrate on the reduction kinetics of Re(VII) in ZVI

1.8 References

Allen P., Siemering G., Shuh D., Bucher J., Edelstein N., Langton C., Clark S., Reich T. and Denecke M. (1997) Technetium speciation in cement waste forms determined by X-ray absorption fine structure spectroscopy. *Radiochim. Acta* **76,** 77-86.

Almond P., Kaplan D., Langton C., Stefanko D., Spencer W., Hatfield A. and Arai Y. (2012) Method evaluation and field sample measurements for the rate of movement of the oxidation front in saltstone. Savannah River National Laboratory. SRNL-STI-2012-00468.

Angus M. J. and Glasser F. P. (1985) The chemical environment in cement matrices. *MRS Online Proceedings.* Cambridge University Press. **50,** 547-556.

Arai Y., Elzinga E. and Sparks D. (2001) X-ray absorption spectroscopic investigation of arsenite and arsenate adsorption at the aluminum oxide-water interface. *J. Colloid Interface Sci.* **235,** 80-88.

Atkins M. and Glasser F. P. (1992) Application of Portland cement-based materials to radioactive waste immobilization. *Waste Manage.* **12,** 105-131.

Bard A. J., Parsons R. and Jordan J. (1985) *Standard potentials in aqueous solution.* CRC press.

Bothe J. and Brown P. (1999) Arsenic immobilization by calcium arsenate formation. *Environ. Sci. Technol.* **33,** 3806-3811.

Brown S., Chaney R., Hallfrisch J., Ryan J. and Berti W. (2004) In situ soil treatments to reduce the phyto- and bioavailability of lead, zinc, and cadmium. *J. Environ. Qual.* **33,** 522-531.

Buj I., Torras J., Rovira M. and de Pablo J. (2010) Leaching behaviour of magnesium phosphate cements containing high quantities of heavy metals. *J. Hazard. Mater.* **175,** 789-794.

Cantrell K. J. and Williams B. D. (2013) Solubility control of technetium release from Saltstone by $TcO_2 \cdot xH_2O$. *J. Nucl. Mater.* **437,** 424-431.

Chen Q. Y., Hills C. D., Tyrer M., Slipper I., Shen H. G. and Brough A. (2007) Characterisation of products of tricalcium silicate hydration in the presence of heavy metals. *J. Hazard. Mater.* **147,** 817-825.

Chen Q. Y., Tyrer M., Hills C. D., Yang X. M. and Carey P. (2009) Immobilization of heavy metal in cement-based solidification/stabilization: A review. *Waste Manage.* **29,** 390-403.

Cobble J. W., Smith W. T. and Boyd G. E. (1953) Thermodynamic Properties of Technetium and Rhenium Compounds. II. Heats of Formation of Technetium Heptoxide and Pertechnic Acid, Potential of the Technetium-(IV)-Technetium(VII) Couple, and a Potential Diagram for Technetium1,2. *J. Am. Chem. Soc.* **75,** 5777-5782.

Cocke D. (1990) The Binding Chemistry and Leaching Mechanisms of Hazardous Substances in Cementitious Solidification Stabilization Systems. *J. Hazard. Mater.* **24,** 231-253.

Conner J. and Hoeffner S. (1998) A critical review of stabilization/solidification technology. *Crit. Rev. Environ. Sci. Technol.* **28,** 397-462.

Cui D. and Eriksen T. (1996) Reduction of pertechnetate by ferrous iron in solution: Influence of sorbed and precipitated Fe(II). *Environ. Sci. Technol.* **30,** 2259-2262.

Deja J. (2002) Immobilization of Cr6+, Cd2+, Zn2+ and Pb2+ in alkali-activated slag binders. *Cem. Concr. Res.* **32,** 1971-1979.

Ding Q., Qian T., Yang F., Liu H., Wang L., Zhao D. and Zhang M. (2013) Kinetics of Reductive Immobilization of Rhenium in Soil and Groundwater Using Zero Valent Iron Nanoparticles. *Environ. Eng. Sci.* **30,** 713-718.

Ebbing D. D. and Wrighton M.S. (1993) *General Chemistry, 4th edition.* Houghton Mifflin, Boston.

Fernandez J. M., Navarro-Blasco I., Duran A., Sirera R. and Alvarez J. I. (2014) Treatment of toxic metal aqueous solutions: Encapsulation in a phosphate-calcium aluminate matrix. *J. Environ. Manage.* **140,** 1-13.

Gauthier-Lafaye F., Holliger P. and Blanc P. (1996) Natural fission reactors in the Franceville basin, Gabon: A review of the conditions and results of a "critical event" in a geologic system. *Geochim. Cosmochim. Acta* **60,** 4831-4852.

Gilliam T., Spence R., Bostick W. and Shoemaker J. (1990) Solidification Stabilization of Technetium in Cement-Based Grouts. *J. Hazard. Mater.* **24,** 189-197.

Glasser F. P. (1997) Fundamental aspects of cement solidification and stabilisation. *J. Hazard. Mater.* **52,** 151-170.

Gollmann M. A. C., da Silva M. M., Masuero A. B. and dos Santos J. H. Z. (2010) Stabilization and solidification of Pb in cement matrices. *J. Hazard. Mater.* **179,** 507-514.

Harbour J., Hansen E., Edwards T., Williams V., Eibling R., Best D. and Missimer D. (2006) *Characterization of slag, fly ash and portland cement for saltstone.* United States Department of Energy Report WSRC-TR-2005-00067.

He Y., Chen C. and Traina S. (2004) Inhibited Cr(VI) reduction by aqueous Fe(II) under hyperalkaline conditions. *Environ. Sci. Technol.* **38,** 5535-5539.

He Y. and Traina S. (2005) Cr(VI) reduction and immobilization by magnetite under alkaline pH conditions: The role of passivation. *Environ. Sci. Technol.* **39,** 4499-4504.

Hidalgo A., Petit S., Garcia J. L., Alonso C. and Andrade C. (2007) Microstructure of the system calcium aluminate cement-silica fume: application in waste immobilization. *From Zeolites to Porous Mof Materials: the 40th Anniversary of International Zeolite Conference, Proceedings of the 15th International Zeolite Conference* **170,** 1617-1628.

Hong S. and Glasser F. (2002) Alkali sorption by C-S-H and C-A-S-H gels - Part II. Role of alumina. *Cem. Concr. Res.* **32,** 1101-1111.

Hsi C. and Langmuir D. (1985) Adsorption of Uranyl onto Ferric Oxyhydroxides - Application of the Surface Complexation Site-Binding Model. *Geochim. Cosmochim. Acta* **49,** 1931-1941.

Icenhower J. P., Qafoku N. P., Zachara J. M. and Martin W. J. (2010) The Biogeochemistry of Technetium: a Review of the Behavior of an Artificial Element in the Natural Environment. *Am. J. Sci.* **310,** 721-752.

Kaplan D. I., Lilley M. S., Almond P. M. and Powell B. A. (2011) Long-Term Technetium Interactions with Reducing Cementitious Materials. Savannah River National Laboratory. SRNL-STI-2010-00668

Kaplan D. I. (2003) Estimated Duration of the Subsurface Reducing Environment Produced by the Z-Area Saltstone Disposal Facility. WSRC-RP_2003-00362, Westinghouse Savannah River Company, Aiken, South Carolina

Kindness A., Macias A. and Glasser F. P. (1994) Immobilization of chromium in cement matrices. *Waste Manage.* **14,** 3-11.

Kumpiene J., Lagerkvist A. and Maurice C. (2008) Stabilization of As, Cr, Cu, Pb and Zn in soil using amendments - A review. *Waste Manage.* **28,** 215-225.

Langton C. A. (1987) Slag-Based Saltstone Formulations. *MRS Online Proceedings*. Cambridge University Press. **112,** 61-70.

Li X., Poon C., Sun H., Lo I. and Kirk D. (2001) Heavy metal speciation and leaching behaviors in cement based solidified/stabilized waste materials. *J. Hazard. Mater.* **82,** 215-230.

Liu H., Qian T. and Zhao D. (2013) Reductive immobilization of perrhenate in soil and groundwater using starch-stabilized ZVI nanoparticles. *Chin. Sci. Bull.* **58,** 275-281.

Lukens W. W., McKeown D. A., Buechele A. C., Muller I. S., Shuh D. K. and Pegg I. L. (2007) Dissimilar behavior of technetium and rhenium in borosilicate waste glass as determined by X-ray absorption spectroscopy. *Chem. Mat.* **19,** 559-566.

Luykx F. (1986) *Technetium in the Environment* (eds. G. Desmet and C. Myttenaere). Springer, Netherlands.

Mallampati S. R., Mitoma Y., Okuda T., Sakita S. and Kakeda M. (2013) Total immobilization of soil heavy metals with nano-Fe/Ca/CaO dispersion mixtures. *Environ. Chem. Lett.* **11,** 119-125.

Malviya R. and Chaudhary R. (2006) Factors affecting hazardous waste solidification/stabilization: A review. *J. Hazard. Mater.* **137,** 267-276.

Mattigod S. V., Wellman D. M., Cordova E. A., Bovaird C. C., Skinner D. and Wood M. I. (2009) *Effect of Concrete Waste Form Properties on Radionuclide Migration.* Pacific Northwest National Laboratory. PNNL-18745.

Miretzky P. and Fernandez-Cirelli A. (2008) Phosphates for Pb immobilization in soils: a review. *Environ. Chem. Lett.* **6,** 121-133.

Momoshima N., Sayad M. and Takashima Y. (1995) Determination of Tc-99 in coastal seawater collected in Fukuoka, Japan. *J. Radioanal. Nucl. Chem. -Artic.* **197,** 245-251.

Momoshima N., Sayad M., Yamada M., Takamura M. and Kawamura H. (2005) Global fallout levels of Tc-99 and activity ratio of Tc-99/Cs-137 in the Pacific Ocean. *J. Radioanal. Nucl.* **266,** 455-460.

Moon D. H., Grubb D. G. and Reilly T. L. (2009) Stabilization/solidification of selenium-impacted soils using Portland cement and cement kiln dust. *J. Hazard. Mater.* **168,** 944-951.

Moon D. and Dermatas D. (2006) An evaluation of lead leachability from stabilized/solidified soils under modified semi-dynamic leaching conditions. *Eng. Geol.* **85,** 67-74.

Moon D., Dermatas D. and Menounou N. (2004) Arsenic immobilization by calcium-arsenic precipitates in lime treated soils. *Sci. Total Environ.* **330,** 171-185.

Mulligan C. N., Yong R. N. and Gibbs B. F. (2001) Remediation technologies for metal-contaminated soils and groundwater: An evaluation. *Eng. Geol.* **60,** 193-207.

Navarro-Blasco I., Duran A., Sirera R., Fernandez J. M. and Alvarez J. I. (2013) Solidification/stabilization of toxic metals in calcium aluminate cement matrices. *J. Hazard. Mater.* **260,** 89-103.

Paria S. and Yuet P. K. (2006) Solidification-stabilization of organic and inorganic contaminants using portland cement: a literature review. *Env. Rev.* **14,** 217-255.

Peters R. (1999) Chelant extraction of heavy metals from contaminated soils. *J. Hazard. Mater.* **66,** 151-210.

Pierce E. M., Mattigod S. V., Westsik J. H., Serne R. J., Icenhower J. P., Scheele R. D., Um W. and Qafoku N. (2010) *Review of Potential Candidate Stabilization Technologies for Liquid and Solid Secondary Waste Streams.* Pacific Northwest National Laboratory, PNNL-19122.

Pollard S., Montgomery D., Sollars C. and Perry R. (1991) Organic-Compounds in the Cement-Based Stabilization - Solidification of Hazardous Mixed Wastes - Mechanistic and Process Considerations. *J. Hazard. Mater.* **28,** 313-327.

Qian G., Sun D. and Tay J. (2003a) Characterization of mercury- and zinc-doped alkali-activated slag matrix - Part I. Mercury. *Cem. Concr. Res.* **33,** 1251-1256.

Qian G., Sun D. and Tay J. (2003b) Characterization of mercury- and zinc-doped alkali-activated slag matrix - Part II. Zinc. *Cem. Concr. Res.* **33,** 1257-1262.

Querol X., Alastuey A., Moreno N., Alvarez-Ayuso E., Garcia-Sanchez A., Cama J., Ayora C. and Simon M. (2006) Immobilization of heavy metals in polluted soils by the addition of zeolitic material synthesized from coal fly ash. *Chemosphere* **62,** 171-180.

Radioisotope safety. (2013) Radioisotope Safety Data Sheet: Technetium-99m. University of Queensland, OHS Division.

Roy A. (2009) Sulfur speciation in granulated blast furnace slag: An X-ray absorption spectroscopic investigation. *Cem. Concr. Res.* **39,** 659-663.

Schulte E. and Scoppa P. (1987) Sources and Behavior of Technetium in the Environment. *Sci. Total Environ.* **64,** 163-179.

Schwochau K. (2000) *Technetium: chemistry and radiopharmaceutical applications*. Wiley-VCH, Weinheim.

Shi K., Hou X., Roos P. and Wu W. (2012) Determination of technetium-99 in environmental samples: A review. *Anal. Chim. Acta* **709,** 1-20.

Singh T. and Pant K. (2006) Solidification/stabilization of arsenic containing solid wastes using portland cement, fly ash and polymeric materials. *J. Hazard. Mater.* **131,** 29-36.

Smith R. W. and Walton J. C. (1992) The Role of Oxygen Diffusion in the Release of Technetium from Reducing Cementitious Waste Forms. *MRS Online Proceedings* **294,** 247-253.

Srivastava S., Gupta V. and Mohan D. (1997) Removal of lead and chromium by activated slag - A blast-furnace waste. *J. Environ. Eng. -ASCE* **123,** 461-468.

Sundaram S., Chun J., Um W., Parker K., Chung C., Westsik Jr J., Valenta M., Kimura M., Pitman S. and Burns C. (2011) Secondary Waste Form Development and Optimization—Cast Stone. Pacific Northwest National Laboratory. PNNL-20159, Rev 1.

Tagami K. (2003) Technetium-99 Behavior in the Terrestrial Environment; Field Observations and Radiotracer Experiments. *Journal of Nuclear and Radiochemical Sciences* **4,** A1-A8.

Tomasevic D. D., Dalmacija M. B., Prica M. D., Dalmacija B. D., Kerkez D. V., Becelic-Tomin M. R. and Roncevic S. D. (2013) Use of fly ash for remediation of metals polluted sediment - Green rernediation. *Chemosphere* **92,** 1490-1497.

Um W., Yang J., Serne J. and Westsik J.H. (2015) Reductive capacity measurement of waste forms for secondary radioactive wastes. *J. Nucl. Mater* **467,** 251-259.

USEPA (2007) Treatment technologies for site cleanup: annual status report (twelfth edition). EPA-542-R-07-012.

USNRC (2005) U.S. Nuclear Regulatory Commission Technical Evaluation Report for the U.S. Department of Energy Savannah River Site Draft Section 3116 Waste Determination for Salt Waste Disposal.

Van Bruwaene R., Hegela M., Gerber G. B., Kirchmann R. and Maisin J. R. (1986) Toxicity of Long-term Application of Dietary Technetium to Rats and their Offspring. In *Technetium in the Environment* (eds. G. Desmet and C. Myttenaere). Springer Netherlands, 391-396.

Vandergraaf T., Ticknor K. and George I. (1984) Reactions between Technetium in Solution and Iron-Containing Minerals under Oxic and Anoxic Conditions. *ACS Symp. Ser.* **246,** 25-43.

Walton J.C., Bin-Shafique S., Smith R.W., Gutierrez N. and Tarquin A. (1997) Role of Carbonation in Transient Leaching of Cementitions Wasteforms. *Environ. Sci. Technol.* **31,** 2345-2349.

Wharton M. J., Atkins B., Charnockab J. M., Livens F. R., Pattrick R. A. D. and Collison D. (2000) An X-ray absorption spectroscopy study of the coprecipitation of Tc and Re with mackinawite (FeS). *Appl. Geochem.* **15,** 347-354.

Wiles C. (1987) A Review of Solidification Stabilization Technology. *J. Hazard. Mater.* **14,** 5-21.

Yeung A. (2010) Remediation Technologies for Contaminated Sites. In *Advances in Environmental Geotechnics* (eds. Y. Chen, L. Zhan and X. Tang). Springer Berlin Heidelberg, 328-369.

Yoshihara K. (1996) Technetium in the environment. In *Technetium and Rhenium Their Chemistry and Its Applications* (eds. K. Yoshihara and T. Omori). Springer Berlin Heidelberg, 17-35.

Yousuf M., Mollah A., Vempati R., Lin T. and Cocke D. (1995) The Interfacial Chemistry of Solidification Stabilization of Metals in Cement and Pozzolanic Material Systems. *Waste Manage.* **15,** 137-148.

Zhou Q., Milestone N. B. and Hayes M. (2006) An alternative to Portland Cement for waste encapsulation - The calcium sulfoaluminate cement system. *J. Hazard. Mater.* **136,** 120-129.

Zhou Y. and Haynes R. J. (2010) Sorption of heavy metals by inorganic and organic components of solid wastes: Significance to use of wastes as low-cost adsorbents and immobilizing agents. *Crit. Rev. Environ. Sci. Technol.* **40,** 909-977.

Chapter 2: Evaluation of Perrhenate Spectrophotometric Methods in Bicarbonate and Nitrate Media

2.1 Abstract

2-pyridyl thiourea and methyl-2-pyridyl ketoxime based perrhenate Re(VII) UV-vis spectrophotometric methods were evaluated in nitrate and bicarbonate solutions ranging from 0.001M to 0.5M. Standard curves at [Re]= 2.5 – 50 mg L^{-1} for the Re(IV)-thiourea and the Re ketoxime complexes were constructed at 405 nm and 490 nm, respectively. Influences of $NaHCO_3$ and $NaNO_3$ concentration on absorbance spectra, absorptivity, and linearity were documented. For both methods, samples in Milli-Q water and $NaHCO_3$ have an R^2 value >0.99, indicating strong linear relationships. Statistical analysis supports that $NaHCO_3$ does not affect linearity between standards for either method. $NaNO_3$ causes major interference with the ketoxime method above 0.001M $NaNO_3$. Data provides information for practical use of Re spectrophotometric methods in environmental media that are high in bicarbonate and nitrate.

2.2 Introduction

Rhenium (Re) is often used as a chemical surrogate of technetium (Tc) because of its similar chemical properties to Tc. In low temperature geochemical environment, both elements are commonly present as tetra and hepta valence state. While the tetravalent state generally forms octahedral structure with oxygen/sulfur atoms, the heptavalent state holds tetrahedral structure with four oxygen atoms. These $Re(VII)O_4^-$ and $Tc(VII)O_4^-$ oxyanions are much more soluble and mobile than Re(IV) and Tc(IV) oxide/sulfides in aquatic and terrestrial environment. A major difference in these elements is that one of Tc isotopes, ^{99}T, is a radioisotope that emits β^-, resulting in the radio activity of 629 kBq/mg (Schwochau, 2000). Technetium-99 has been produced during induced fission of ^{235}U in nuclear reactors, and it has a long half-life of 2.13 x 10^5 yrs. For this reason, it is a major environmental concern at many nuclear facilities in the world. In particular, at the United States nuclear fuel reprocessing plants at the Savannah River Site (SRS) in South Carolina and the Hanford Site (HS) in Washington, over 80 million gallons of high level waste (HLW) from the cold war are currently housed (Lukens et al., 2007). Technetium-99 in this waste has been stored in brine (e.g., high nitrate) and alkaline liquid (Almond et al., 2013). Accurate assessment of aqueous speciation of Tc in this complex aqueous

matrix is critical in suggesting the best remediation/immobilization strategies. There are needs for in-situ analytical method to speciate dissolved Tc in brine and alkaline solutions. While inductively coupled plasma (ICP)-optical emission spectrometry (OES) and ICP-mass spectrometry (MS) can be used to determine total Tc concentration, spectrophotometric methods for Re might have potential in speciating Tc in aqueous media if these methods can overcome the matric effect of high bicarbonate and nitrate.

Early Re spectrophotometric methods were introduced in the 1950's, and have since been further developed by exploring new color forming complexing reagents, and wavenumber ranges from 230 to 650 nm. Common compounds are brilliant green, amiloride hydrochloride, thiocyanate, thiobenzhydrazide, methyl isobutyl ketone, 2-pyridyl thiourea, 4-methylnioxime, and α-furildioxime (Burns and Tungkananuruk, 1988; Burns et al., 1996; Dutta and Sur, 1986; Gangopadhyay et al., 1976; Kassner et al., 1961; Meloche et al., 1957; Poineau et al., 2006; Wahi and Kakkar, 1997). Some methods use hazardous chemicals, such as benzene, and/or involve time-consuming liquid separation steps with organic solvents (Gangopadhyay et al., 1976; Wahi and Kakkar, 1997). The detection limit of these methods is ranging from 0.4 to 10,000 mg L^{-1}. Because of inertness of perrhenate (Re(VII) O_4^-), most of methods involve the reduction of Re(VII) to Re(IV) with reducing agents such as $SnCl_2$ (Dutta and Sur, 1986; Gangopadhyay et al., 1976; Hindman and Wehner, 1953; Kassner et al., 1961; Maun and Davidson, 1950; Meloche et al., 1957; Wahi and Kakkar, 1997), but only few direct analyses of Re(VII) are available without the use of reducing agents (Burns and Tungkananuruk, 1988; Kormosh and Bazel, 1999). These methods are known to obey Beer's law over a wide concentration range (e.g., 0-40 mg L^{-1}). However, these Re spectrophotometric methods have not yet been established for environmental applications since 1) most of the methods involve time consuming phase separation steps with organic solvents and 2) surface and groundwater always contain cations and anions that could potentially interfere with the methods. Only a few studies have evaluated the sensitivity of these spectrophotometric techniques with interfering ions. The thiobenzhydrazide-based method can measure up to ~13 mg L^{-1} of Re as long as [Cu] < 25 mg L^{-1} (Gangopadhyay et al., 1976) while thiocyanate method can detect ~12 mg L^{-1} of Re when a high level (500 mg L^{-1}) of Mo, V and W are present (Gangopadhyay et al., 1976; Savariar and Hariharan, 1975). Agnihotri and co-workers noted that the detection of low (2.5 mg L^{-1}) [Re] is

possible in the diphenylbenzamidine-based method as along as [Mo] <20 mg L^{-1} (Agnihotri et al., 1998).

In order to further validate the reliability of Re spectrophotometric methods for Tc aqueous speciation in caustic and brine liquid waste, it is necessary to evaluate these spectrophotometric methods in nitrate and bicarbonate media. The objective of this study was to evaluate two Re spectrophotometric methods (Dutta and Sur, 1986; Thompson et al., 1964) in the presence of NO_3^- and HCO_3^-. Specifically, the effects of these background solutions on the detection limit, linearity ranges and molar absorptivity were evaluated. These two methods were chosen since they do not involve the time consuming phase separation steps using organic solvents. Therefore they are the most promising methods that can be adapted for the environmental research applications. Both methods involve the reduction of Re(VII)) by a reducing agent, $SnCl_2$, but use different complexing agents N-(2-Pyridyl) thiourea (Dutta and Sur, 1986) and Methyl-2-Pyridyl Ketoxime (Thompson et al., 1964).

2.3 Materials

All reagents were prepared in Mili-Q water (18.2MΩ) using ACS-grade chemicals. A 1000 mg L^{-1} ICP Re(VII) standardized solution in water (Ricca chemical co. Arlington, TX) was used to prepare Re(VII) standards in Mil-Q water and the nitrate or bicarbonate solutions (0.001M, 0.01M, 0.05M, 0.1M, and 0.5M). The concentrations of Re standards are 2.5, 5, 10, 15, 20, 30, 40, and 50 mg L^{-1}.

Two color forming reagents were prepared using the following methods. For the method presented by Dutta and Sur (1986), a 0.03M 2-pyridyl thiourea solution was prepared in 500 mL of ethanol. A diluted ethanol mixture was also prepared by adding 167 mL of Mili-Q water to approximately 333 mL of ethanol. For the method presented by Thompson et al. (1964), a 0.01M Methyl-2-Pyridyl Ketoxime solution was prepared by dissolving 0.681 g in 500 mL of Milli-Q water.

A 0.6M $SnCl_2$ solution was prepared by dissolving $SnCl_2$ anhydrous salts in 1.2M HCl or in 6M HCl using $SnCl_2$ anhydrous salts. It should be noted that many commercial $SnCl_2$ dihydrate salts contain impurities such as a basic tin chloride (Sn(OH)Cl) and a β-stannic acid (SnO_2. xH_2O) that are not soluble in water or in mildly acidic solutions (e.g., 1.2-6 M HCl) at room temperature. If present these impurities give cloudiness in water. There are a few

important steps in making this reagent. For the method by Dutta and Sur (1986), approximately 33 g of $SnCl_2$ was added to 50mL of 6M HCl in a 500mL beaker. The beaker was covered with a watch glass, and the contents boiled for 45-60 min. The solution should become clear or a transparent light yellowish color. And then 200mL Mil-Q water was added to make the final concentration of $SnCl_2$ and HCl to 0.6 and 1.2M, respectively. For the method by Thompson et al. (1964), the same boiling process was repeated but it was followed by dilutions with 200 mL of 6M HCl solution instead of 200 mL of Mil-Q water. This gave a 0.6M $SnCl_2$ solution in 6M HCl for the second method.

During boiling, if the solution becomes cloudy, Sn(OH)Cl(s) and $SnO_2.xH_2O$(s) impurities are still present. At this point, a new batch of $SnCl_2$ solution should be prepared with sufficient boiling time (>60min) in a 6M HCl solution. It might be also useful to use anhydrous $SnCl_2$ since this contains near negligible amounts of Sn(OH)Cl(s) and $SnO_2 \cdot xH_2O$(s) impurities. Since $SnCl_2$ is sensitive to oxidation by contact with air (Nechamkin, 1968), it was prepared freshly for every use. Shelf life of this solution under ambient condition is about 4 days.

Because of lack of description in the previous works, the thermodynamic calculation of reduction of Re(VII) to Re(IV) by Sn(II) was summarized below. Shown below is a combination of half reactions provided by Bard et al., (1985).

$$ReO_4^- + 4H^+ + 3e^- \rightarrow ReO_2 + 2H_2O \qquad E^\circ = 0.51\ V$$

$$Sn^{4+} + 2e^- \rightarrow Sn^{2+} \qquad E^\circ = 0.15\ V$$

Combining the two half reactions yields the following overall reaction,

$$ReO_4^- + 4H^+ + 1.5\ Sn(II) \rightarrow ReO_2 + 1.5\ Sn(IV) + 2H_2O$$

$$\Delta G^\circ = -212.75\ kJ/mol$$

This overall reaction suggests that [Sn(II)Cl_2] should be 1.5 times greater than [Re(VII)] if there are no interferences. In our study, the maximum concentrations of Re standard is 7.99 x 10^{-5} M (20 mg L^{-1}). Therefore, a 0.6 M of Sn(II)Cl_2 reagent should be sufficient to reduce

Re(VII). However, it should be noted that $SnCl_2$ is in excess in case it interferes with the background solutions being tested.

In summary, the following three reagents were made for the method by Dutta and Sur (1986): 0.6 M of $Sn(II)Cl_2$ reagent in 1.2M HCl, 0.03M 2-pyridyl thiourea solution in ethanol, diluted ethanol mixture (167 mL of Milli-Q water and 333 mL of ethanol). For the method presented by Thompson et al. (1964), three reagents were prepared: 0.6 M of $Sn(II)Cl_2$ in 6M HCl, 6M HCl and 0.01M methyl-2-pyridyl ketoxime solution in Mil-Q water.

2.4 Methods

All measurements were performed in triplicates for each set of standards in 0.001M – 0.5M nitrate and carbonate background solutions.

For the N-(2-pyridyl) thiourea method by Dutta and Sur (1986), 2 mL of a Re standard was mixed with 3 mL of 0.03M 2-Pyridyl Thiourea, 1 mL 0.6M $Sn(II)Cl_2$ solution, 0.5 mL of 6M HCl, and 3.5 mL of the diluted ethanol mixture. Addition of 6M HCl was necessary to maintain acidic pH. The measured pH range of the samples was 0.75±0.05. The solution was mixed and allowed to stand for ~2.5 hrs. in order for a yellow-beige color to fully develop (Fig. 2.1). Although the original N-(2-Pyridyl) thiourea method specified a period of 15-20 min to form color, our preliminary experiments suggested that the method requires 2.5-3 hrs to fully develop the Re(IV)- N-(2-Pyridyl) thiourea complex (Fig. 2.2). After color development, absorbance was recorded at 405 nm in 1cm cuvettes against a reagent blank prepared under the same conditions using a Flame® spectrophotometer unit (Ocean Optics Inc. Dunedin, FL) equipped with a DT-MINI-2 Deuterium Tungsten Halogen Light Source. Ten scans were averaged under the following scan parameters (integration time: 12 ms and boxcar width: 5) using Ocean optics software, Oceanview®. To monitor the shift in peak maxima, absorbance spectra were also recorded for 350-800nm.

For the methyl-2-pyridyl ketoxime method by Thompson et al. (1964), 2 mL of each Re sample or standard was mixed with 2 mL of 0.01M Methyl-2-pyridyl ketoxime solution, 1 mL of 0.6M $Sn(II)Cl_2$ solution prepared in 6M HCl, and 2 mL of 6M HCl. The measured pH range of the samples was 0.24±0.10. As the original paper indicated, the acidity in this method seems critical for proper color development. An addition of 2mL $\geq$ 6M HCl is needed to develop purple color (Fig. 2.3). The color of Re(IV)-methyl-2-pyridyl ketoxime complex (Fig. 2.4) was allowed to

form for 1hr and absorbance was measured at 490 and 630 nm against a blank prepared under identical conditions. The color is stable for 24hrs. The measurements were repeated in bicarbonate and nitrate background electrolyte media like the first method. Absorbance spectra were also recorded for 350-800 nm.

Spectra features, peak maxima, and absorbance intensity were then evaluated for differences in detection limits and linearity ranges for Re concentrations within each background solution, with respect to Milli-Q background.

2.5 Results and Discussion

N-(2-Pyridyl) thiourea based method

Fig. 2.5A shows absorption spectra of Re-complex in Mili-Q water. From thereafter, mil-Q-water system is referred as a control system unless otherwise mentioned in text. Observed absorbance reported by Dutta and Sur (1986) was at 405 nm. An absorbance slightly shifts from 405 to 403nm with increasing [Re]. At [Re] of 2.5 – 10 mg L^{-1}, $\lambda_{max} \sim 403$ nm. With increasing [Re] to 50 mg L^{-1}, λ_{max} continues to shift to 380 nm. This wavelength can be appropriate at high [Re] (i.e., > 50 mg L^{-1}) due to the broad nature of the peaks. According to the original method by Dutta and Sur (1986), a standard curve was constructed using absorbance data collected at 405 nm. The linear regression line has an R^2 value of 0.9943, indicating a strong linear relationship (Table 2.1). The intensity of a light yellow/brown or beige color increases with increasing [Re] (Fig. 2.1).

Maximum absorbance also shifts with increasing [Re] in the $NaHCO_3$ background solutions (Figs. 2.6A, 2.6B, 2.6C and 2.6D). Absorbance in low [Re] (2.5 and 5 mg L^{-1}) samples is shifted to slightly lower wavelengths to 400 nm in 0.01M to 0.1M $NaHCO_3$. Re concentrations ranging from 30 – 50 mg L^{-1} all have a $\lambda_{max} = 390$ nm. The observation was consistent in 0.5M $NaHCO_3$ background solution (not shown). Other than Re concentration, all factors within each $NaHCO_3$ background and Mili-Q water were held constant. The color formed was similar to the control samples, and no visual differences could be noticed.

Figs. 2.7A-2.7D show absorbance spectra within [$NaNO_3$] of 0.001M, 0.01M, 0.05M, and 0.1M respectively. An absorbance shift is apparent with increasing $NaNO_3$ concentration, which moves further into the UV region. At a Re concentration of 50 mg L^{-1}, an absorbance peak is present at 385 nm in the 0.001M $NaNO_3$ background. The peak continues to shift to a lower

wavelength at 360 nm in the 0.1M $NaNO_3$ background and 355 nm in 0.5M $NaNO_3$. This characteristic was not mentioned in the original paper, and nitrate was not reported to interfere with the colored complex. Despite the absorbance spectra being shifted, the visual color remains the same color at all [Re], but only slightly paler than observed in the Mili-Q background.

There is minimal information available in the literature regarding nitrate complexing with thiourea. However, a number of ions have strong absorption values in the UV region, some of which are both nitrate and nitrite (Sommer, 1989). This could possibly be why absorption peaks shift further into the UV region with increasing $NaNO_3$ background concentration caused by nitrate interference with the method. In acidic solution, it has been suggested that nitrous acid can form, which has been shown to have an absorption peak at 355 nm (Altshuller and Wartburg, 1960; Wetters and Uglum, 1970). Based on thermodynamic calculations, formation of nitrous acid from the reduction of NO_3^- by $SnCl_2$ in acidic solution has a Gibbs free energy value of -210.338 kJ/mol. The reaction is shown below, half reaction potentials in acidic solution are taken from Bard et al., (1985).

$$NO_3^- + 3H^+ + 2e^- \rightarrow HNO_2 + H_2O \qquad E^0 = 0.94\,V$$

$$Sn^{4+} + 2e^- \rightarrow Sn^{2+} \qquad E^0 = 0.15\,V$$

$$NO_3^- + 3H^+ + Sn(II) \rightarrow HNO_2 + Sn(IV) + H_2O$$

$$\Delta G = -210.338\,kJ/mol$$

Due to reaction favorability and excess $SnCl_2$ in the system, it seems reasonable that interference could be caused by this nitrate reducing causing the absorbance peak to shift further into the UV region. Nitrate itself been measured even further into the UV region, at 220 nm (Collos et al., 1999; Finch et al., 1998). Reduction of nitrate to form nitrite by $SnCl_2$ has a Gibbs free energy value of -215.162 kJ/mol, which is also favorable. The reaction is shown below.

$$NO_3^- + 2H^+ + 2e^- \rightarrow NO_2^- + H_2O \qquad E^0 = 0.965\,V$$ (Plieth, 1973)

$$Sn^{4+} + 2e^- \rightarrow Sn^{2+} \qquad E^0 = 0.15\ V$$

$$NO_3{}^- + 2H^+ + Sn(II) \rightarrow NO_2{}^- + Sn(IV) + H_2O$$

$$\Delta G = -215.162\ kJ/mol$$

Table 2.1 summarizes absorptivity and R^2 values for all Re concentrations. This information indicates a strong linear relationship for each of the tested reaction conditions. Beer's law is obeyed over the full range of Re concentrations for each background solution represented by the strong linear relationship among the range of standards. Compared to the absorptivity in the control system, it decreases with increasing $NaNO_3$ concentration, ranging from 0.0049 at 0.001M $NaNO_3$ to 0.0027 at 0.5M $NaNO_3$. Based on the linear relationships, it should be suitable to determine Re concentration. However it is important to note that 2.5 mg L^{-1} Re in 0.5M $NaNO_3$ was below detection limit.

A statistical analysis was performed by using a t-test at an alpha value of 0.01 to evaluate differences between absorptivity and R^2 values with respect to the control. None of the R^2 values for both $NaHCO_3$ and $NaNO_3$ were significantly different from the control system. Absorptivity in the $NaNO_3$ background series decreased significantly with increasing $NaNO_3$ concentration, whereas absorptivity showed no statistically significant change with addition of $NaHCO_3$.

Although it was suggested in the original method, linear regression analysis at observed peak maxima < 405nm were attempted. Table 2.2 summarizes linear absorptivity and R^2 values for Re standards that share the same absorbance maximum for Mili-Q, $NaHCO_3$, and $NaNO_3$ background. Some ranges are not available because only two or fewer Re standards shared an absorbance maximum, therefore a standard curve could not be constructed. In most cases, using the absorbance maximum results in a lower R^2 value than using 405 nm as mentioned in the original paper. This is especially noticeable in the 0.5M $NaNO_3$ background, which has an absorbance maximum at 355 nm and an R^2 value of 0.9407. Using 405 nm to construct a curve gives a much more linear relationship than using absorbance maxima for this background solution, and therefore is more appropriate to determine unknown amounts of Re over the entire range.

Methyl-2-Pyridyl Ketoxime based method

Fig. 2.5B shows that a standard curve based on the original method described by Thompson and co-workers (1964). The concentration range of 2.5-50 mg/L was tested in our experiment. As the original paper described, a linear range of >0.99 was obtained at two different wavenumbers (490 and 630nm) (Table 2.3).

Absorption spectra in a control system are shown in Fig. 2.3B. With increasing Re concentration from 2.5 – 50 mg/L, two peaks are apparent at 490 nm and 630 nm. This agrees with the observation reported by Thompson et al. (1964). The absorbance peak at 490 nm has a higher absorbance value than the longer wavelength peak at 630 nm. The R^2 value was 0.9969 at the 490 nm absorbance peak and 0.9968 at the 630 nm peak, which indicates a strong linear relationship and that Beer's law is obeyed within this concentration range at both of these wavelengths.

The complex formed a green color after allowing appropriate time for purple color development (Fig. 2.3). After 30 minutes, the color complex formed, and it was stable for at least 24 hrs. In this method, each sample contains 2.58M HCl. If the acidity is below this level, purple color quickly fades to brown. The color complex formed would not be stable enough to take accurate absorbance measurements. For this reason, it is important to ensure that the sample is acidic enough to facilitate color stability and for accurate measurements.

Figs 2.8A-2.8D show absorption spectra in 0.001M, 0.01M, 0.05M, and 0.1M $NaHCO_3$ background solutions, respectively. The absorbance peaks remain consistent for each concentration of $NaHCO_3$ and also for each Re standard concentration within a given background. Also, minimal sensitivity for lower Re concentrations is lost with increasing $NaHCO_3$ concentration. The spectra in the 0.5M $NaHCO_3$ solution (not shown) are similar to Fig. 2.8D, showing the large interference from the high nitrate media. This relationship suggests that this method is only suited for spectrophotometric analysis of Re with $NaHCO_3$ concentrations up to at least 0.5M. Rhenium samples in $NaHCO_3$ also formed a green complex with the color forming reagent, and no visual differences could be noticed, and no shifts in absorbance peaks occurred.

Fig. 2.9A-2.9D shows absorption spectra for $NaNO_3$ backgrounds of 0.001M, 0.01M, 0.05M, and 0.1M, respectively. With increasing $NaNO_3$ concentration, sensitivity and detection ability for Re begins to diminish. The 0.5M $NaNO_3$ background absorbance spectra are not

shown because it was below detection limit. At 0.01M, absorbance peaks begins to shift. The absorbance peak at 630 nm becomes larger in relation to the peak at 490 nm. This characteristic is opposite to that observed for the control system, where the 490 nm peak had comparatively higher absorbance than the 630 nm peak. Therefore, it may be advantageous to use the 630 nm peak in the presence of $NaNO_3$. The peak at 490 nm also begins to shift to slightly smaller wavelengths as $NaNO_3$ increases, whereas the 630 nm peak remains consistent. Absorbance values at 630 nm for 50 mg L^{-1} Re within $NaNO_3$ backgrounds lowers from 0.253, 0.11, 0.034, 0.030, and 0.027 with increasing $NaNO_3$ concentration. Detection range also decreases with increasing $NaNO_3$ concentration. The colored complex formed in the $NaNO_3$ background was more pale green in comparison to the control and $NaHCO_3$ backgrounds.

A summary of detection ranges, absorptivity, and R^2 within the Re standard curves is shown in Table 2.3. The R^2 values for Mili-Q and $NaHCO_3$ standard curves all show a strong linear relationship of values greater than 0.99 for the whole range of Re concentrations that were tested, indicating that Beer's law is also obeyed for all $NaHCO_3$ samples at both absorbance peaks as well. Absorptivity of the colored complex in $NaHCO_3$ varies within a few ten thousandths of a decimal place in comparison to the Mili-Q system for both the 490 nm and 630 nm absorbance peaks and shows no major changes with increasing $NaHCO_3$ concentration. Evidence that is shown here further supports that Re can be accurately determined using this method in systems containing carbonate. However, $NaNO_3$ causes interferences at concentrations greater than 0.001M. Rhenium detection ranges at concentrations greater than 0.01M were lost completely, since many of the spectra lines began to overlap, therefore a standard curve could not be produced. This can result from degradation of the ketoxime complex by nitrous acid produced in solution (Kliegman and Barnes, 1972). Formation of nitrous acid via reduction of NO_3^- by $SnCl_2$ in acidic conditions was shown to be favorable in the thermodynamic calculation presented earlier. This would prohibit the adequate complexation with Re, thus resulting in a loss of color formation.

A t-test was performed to evaluate if there was any statistical difference between the mean absorptivity and R^2 values in Table 2.3 of the Mili-Q system in relation to each of the $NaHCO_3$ and $NaNO_3$ backgrounds by using the three trials performed for each Re standard sample set. This was evaluated for both of the absorbance peaks at 490 nm and 630 nm using an alpha value of 0.01. Analysis showed that none of the average absorptivities and R^2 values for

the $NaHCO_3$ backgrounds was statistically different from the Mili-Q background. This information further supports that $NaHCO_3$ does not affect the accuracy of this method. Absorptivity of 0.001M $NaNO_3$ decreased at 490 nm with respect to the Mili-Q background, but R^2 was not statistically different. The 630 nm showed no statistical differences, and therefore more advantageous to use. Due to the limited detection range of the 0.01M $NaNO_3$ background, it could not be compared to the full concentration range of Mili-Q background. Higher concentrations of $NaNO_3$ were also not appropriate for statistical evaluation because of their severely limited detection ability.

2.6 Conclusion

The two chosen UV-vis Re N-(2-Pyridyl) thiourea based spectrophotometric method (Dutta and Sur, 1986) and Methyl-2-Pyridyl Ketoxime based spectrophotometric method (Thompson et al., 1964) have been evaluated in the presence of $NaHCO_3$ and $NaNO_3$.

For the N-(2-Pyridyl) thiourea method, broad peaks were observed in the 380 – 405 nm region in Mili-Q water, and the color formation required approximately 2.5 hrs. in order to stabilize. The color formed was light yellow/beige and was not stable after ten hours. Addition of $NaHCO_3$ did not cause any major interference, only that the 2.5 mg L^{-1} Re standard was not detected in high 0.5M $NaHCO_3$ concentration. There were no significant differences in linear relationship between standards with increasing $NaHCO_3$ concentration. Addition of $NaNO_3$ resulted in an absorbance peak shift further into the UV region with increasing $NaNO_3$ concentration. Sensitivity for 2.5 mg L^{-1} Re was lost in 0.5M $NaNO_3$ at 405 nm. Construction of a standard curve at the specified 405 nm wavelength had no significant changes in R^2 values with respect to control by increasing [$NaNO_3$].

The methyl-2-pyridyl ketoxime method showed two major absorbance peaks at 490 nm and 630 nm, and formed a green color within 30 min. under acidic conditions (2.58M M HCl) and was stable for 24 hrs. If the sample was not acidic enough, the color faded to a purple and could not be stabilized. With proper acidity, the green colored complex formed was stable for at least 48 hrs. Addition of $NaHCO_3$ caused no interferences with Re analysis. Addition of $NaNO_3$ resulted in major interferences above concentrations of 0.001M, causing limited detection ranges and lowered sensitivity. Absorptivity at the 490 nm peak in 0.001M $NaNO_3$ showed a significant decrease in comparison to the Mili-Q background. The 630 nm peak was unaffected with respect

to the Mili-Q background. This method may not be appropriate for Re analysis in the presence of nitrate above 0.001M concentration.

Information gathered from this study further refines Re spectrophotometric techniques, and offers some potential implications towards the practicality of UV-vis Tc analysis in environmental systems which enriched in nitrate and bicarbonate ions. While it was tested for high brine ^{99}Tc liquid waste, the application can also be extended to typical freshwater and seawaters that have a bicarbonate concentration of 0.0001 - 0.005M (Stumm and Morgan, 1996). In these settings, bicarbonate should not interfere with either method. Nitrate concentration in groundwater can vary greatly. Groundwater and drinking water reservoirs commonly have nitrate concentrations below 45 mg L^{-1} NO_3^- (0.725 mM), which is the maximum contaminant level set by the USEPA (Spalding and Exner, 1993). This concentration is far below the 0.001M limit for the method by Thompson et al. (1964), therefore both tested methods would not be subject to nitrate interferences. Further studies should be conducted using ^{99}Tc analysis in order to continue refining these spectrophotometric techniques in environmental settings.

2.7 Figures

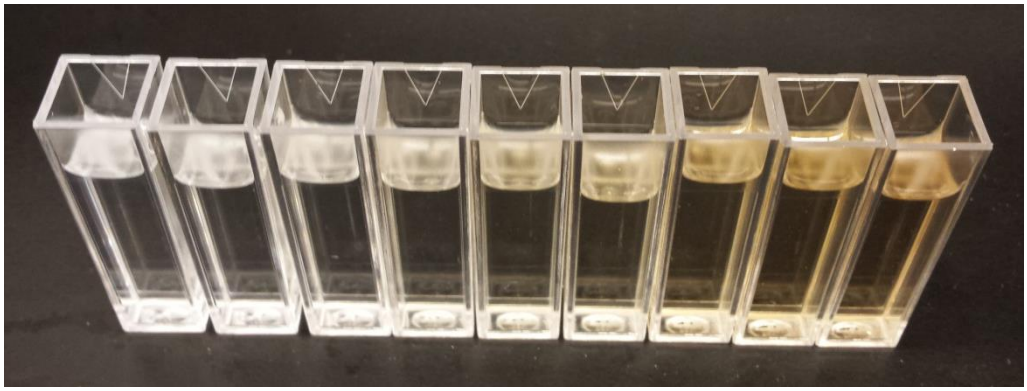

Figure 2.1: Color of Re(IV)-pyridyl thiourea complex as a function of Re(IV) concentration (Dutta and Sur,1986). Concentration is increasing from zero (left), 2.5, 5, 10, 15, 20, 30, 40, to 50 mg L^{-1} (right).

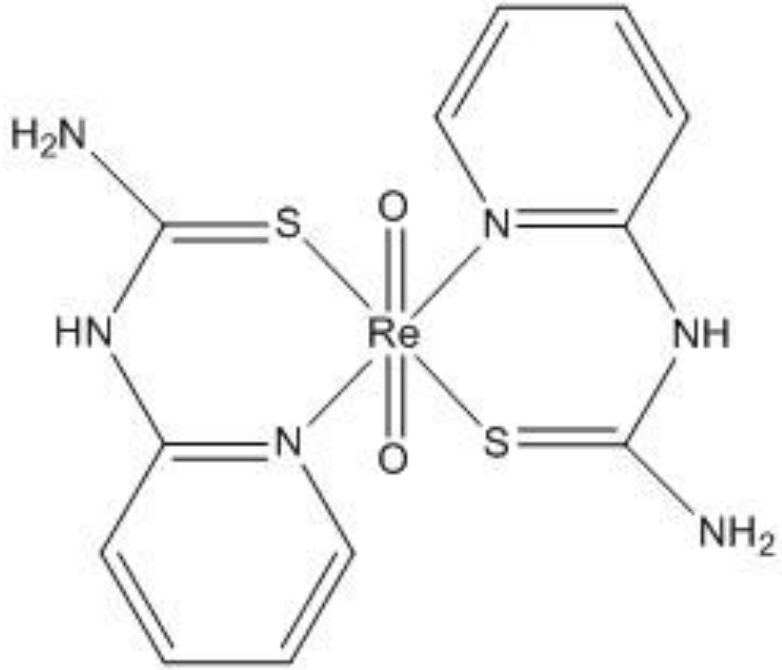

Figure 2.2: Molecular structure of Re(IV)-pyridyl thiourea complex (Dutta and Sur, 1986)

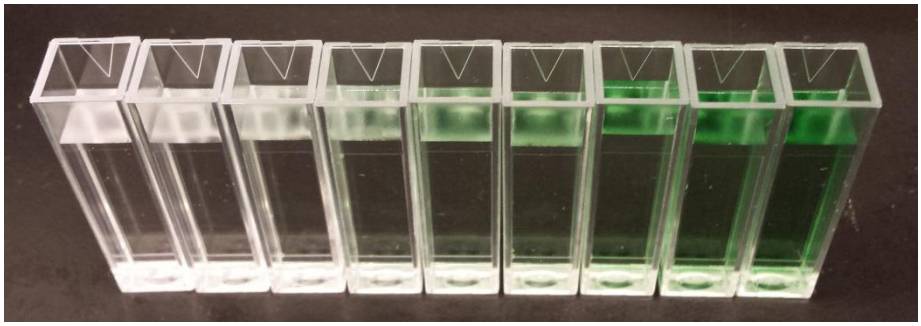

Figure 2.3: Color of Re(IV)- methyl-2-pyridyl ketoxime complex as a function of Re(IV) concentration (Thompson et al., 1964). Concentration is increasing from zero (left), 2.5, 5, 10, 15, 20, 30, 40, to 50 mg L^{-1} (right).

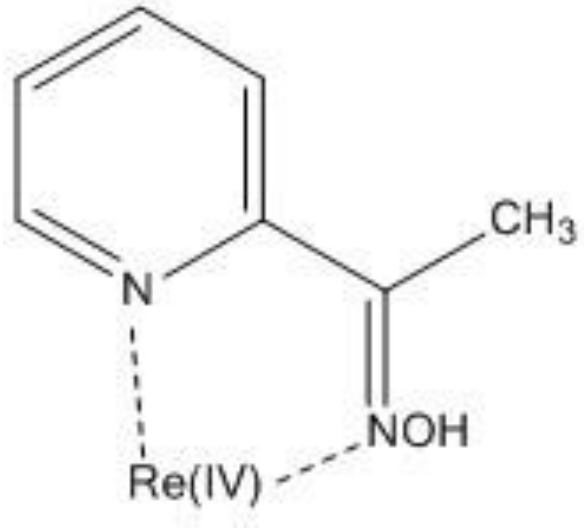

Figure 2.4: Molecular structure of Re(IV)- methyl-2-pyridyl ketoxime complex (Thompson et al., 1964).

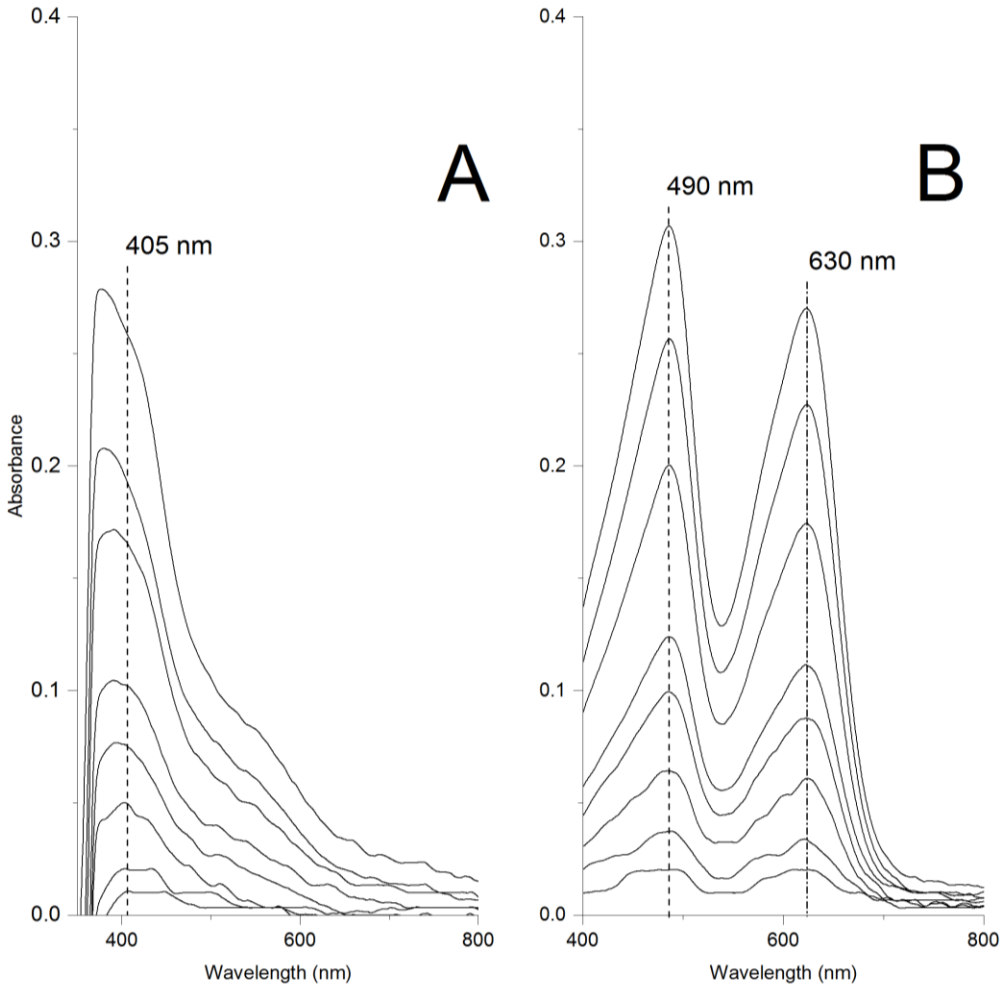

Figure 2.5: Absorbance spectra of (A) Re(IV)-pyridyl thiourea complex (Dutta and Sur, 1986) and (B) Re(IV)- methyl-2-pyridyl ketoxime (Thompson et al., 1964) as a function of Re concentration. The intensity of spectra increases from 2.5 (bottom), 5, 10, 15, 20, 30, 40, to 50 mg L^{-1} (top). Vertical dashed lines are monitored wavelengths (nm) according to the original methods.

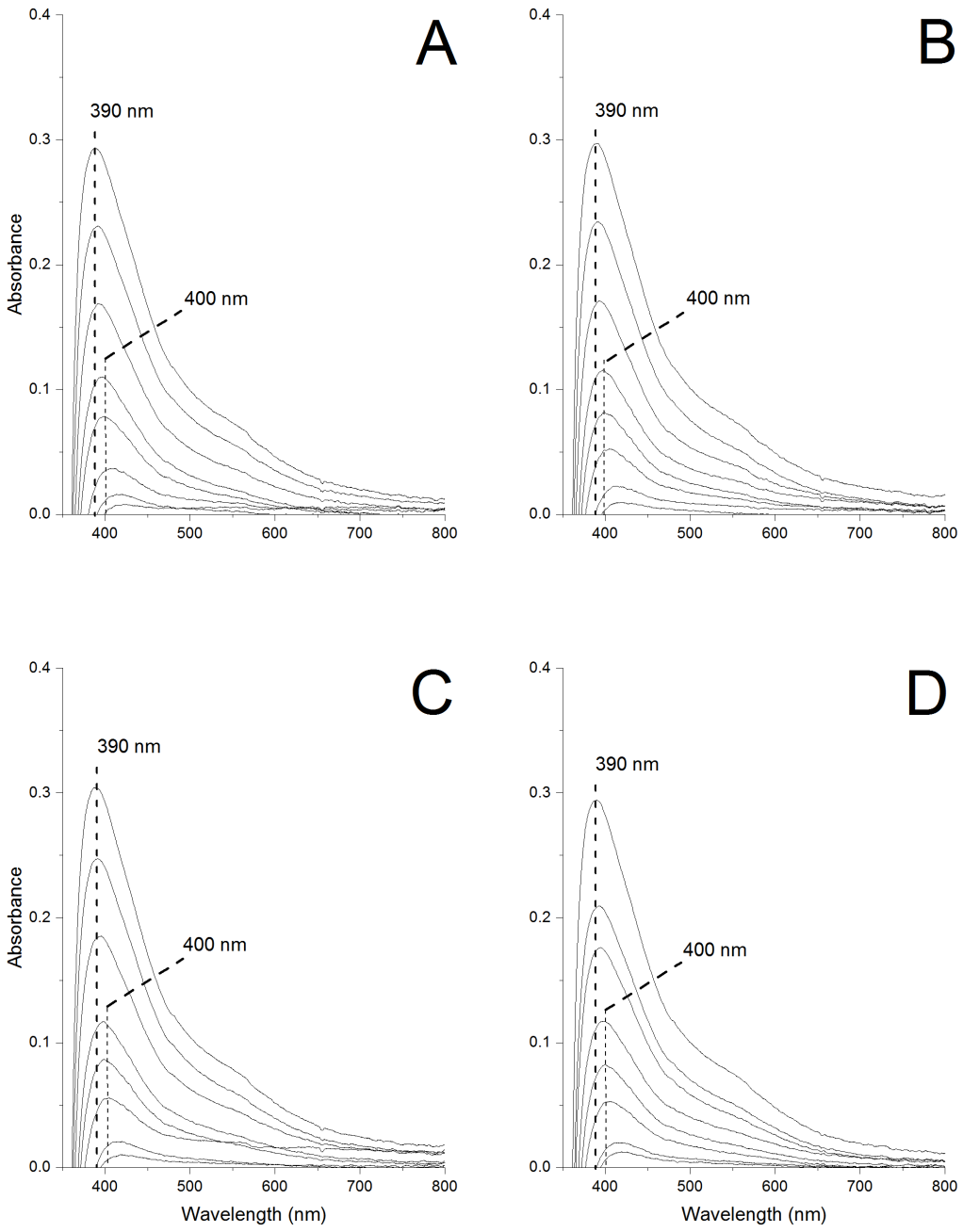

Figure 2.6: Absorbance spectra of Re(IV)-pyridyl thiourea complex (Dutta and Sur, 1986) in $NaHCO_3$ background solutions, A) 0.001M, B) 0.01M, C) 0.05M and D) 0.1M. In each figure, the intensity of spectra increases from 2.5 (bottom), 5, 10, 15, 20, 30, 40, to 50 mg L^{-1} (top) of Re(IV).

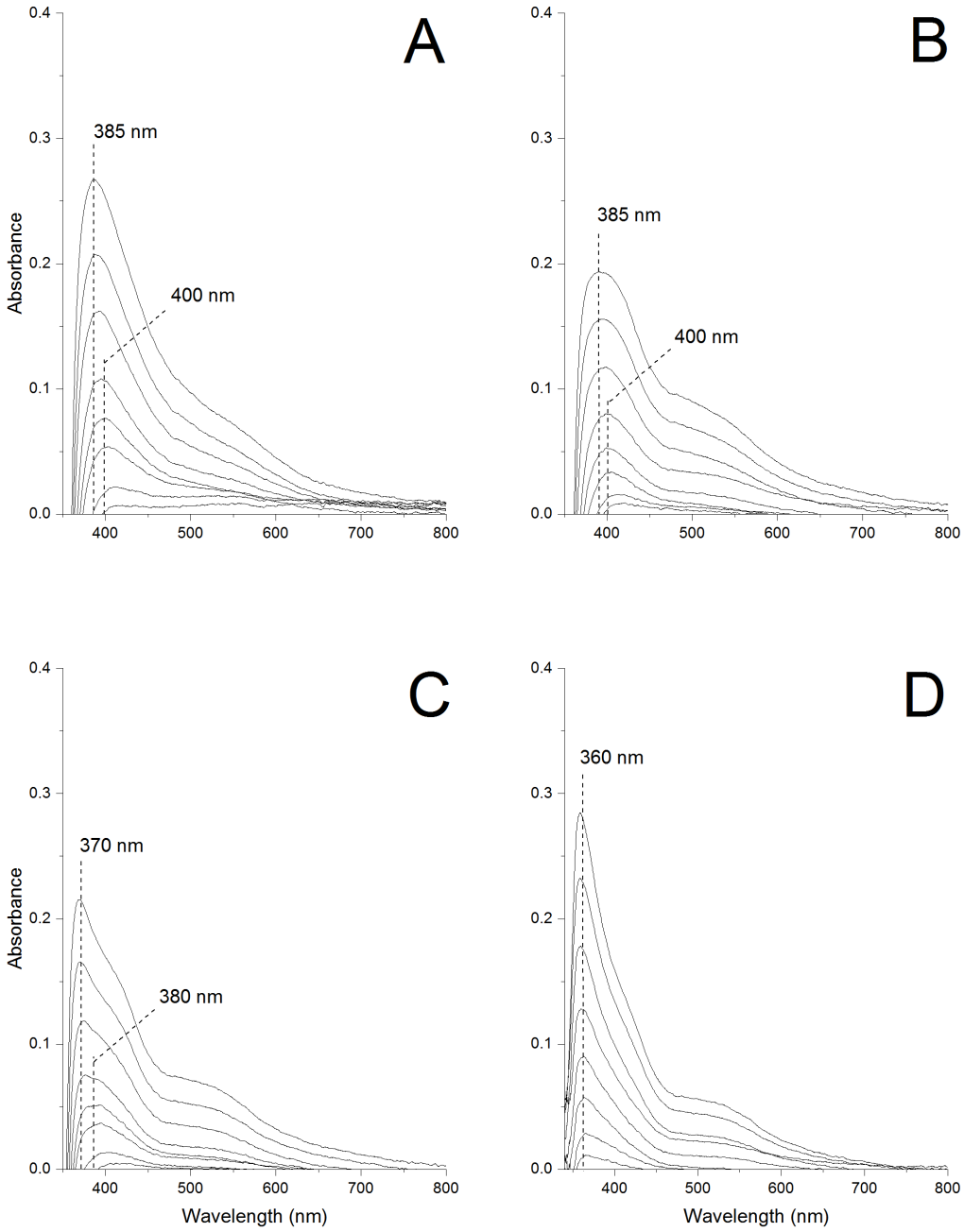

Figure 2.7: Absorbance spectra of Re(IV)-pyridyl thiourea complex (Dutta and Sur, 1986) in $NaNO_3$ background solutions, A) 0.001M, B) 0.01M, C) 0.05M and D) 0.1M. In each figure, the intensity of spectra increases from 2.5 (bottom), 5, 10, 15, 20, 30, 40, to 50 mg L^{-1} (top) of Re(IV).

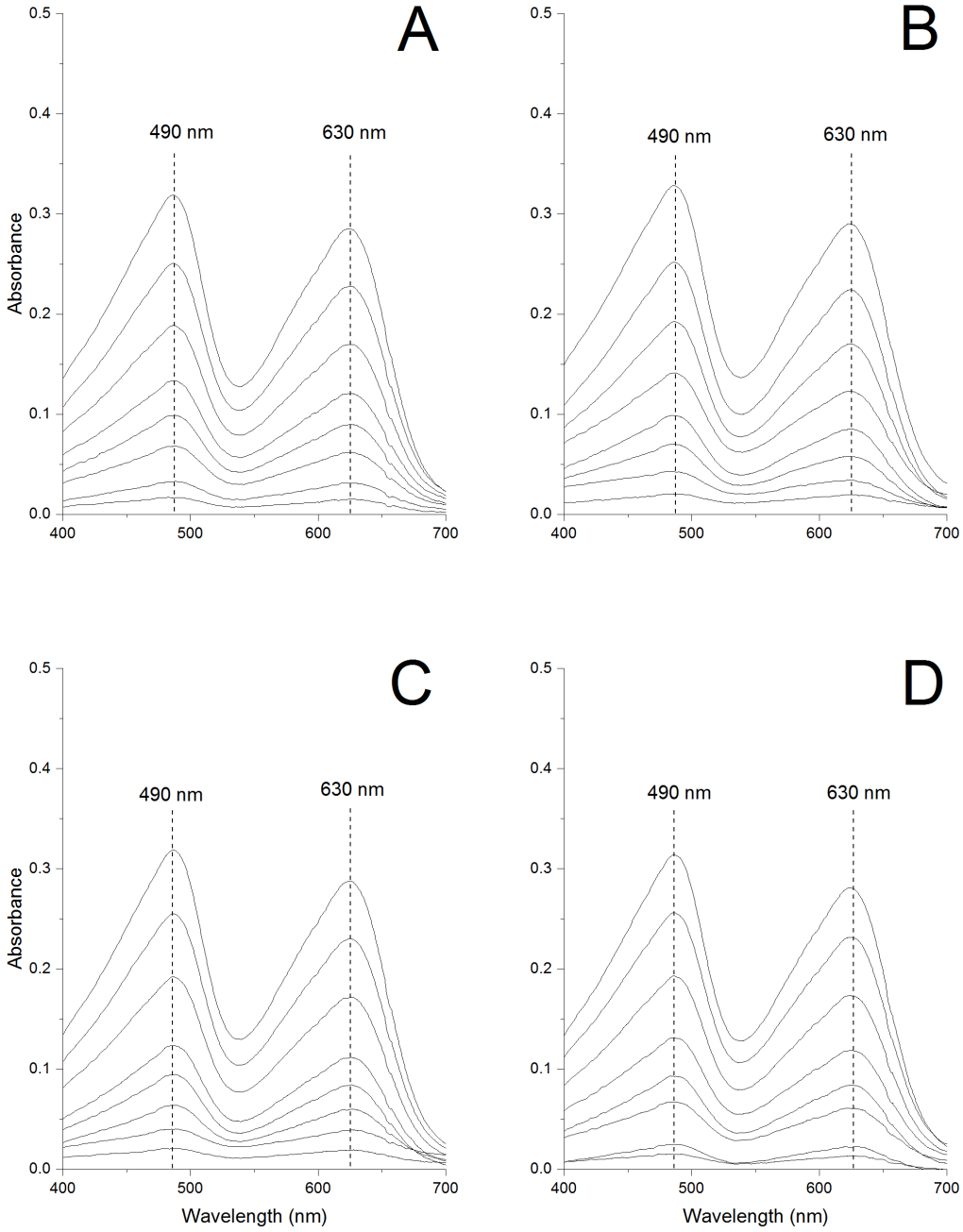

Figure 2.8: Absorbance spectra of Re(IV)-methyl-2-pyridyl ketoxime complex (Thompson et al., 1964) in $NaHCO_3$ background solutions, A) 0.001M, B) 0.01M, C) 0.05M and D) 0.1M. In each figure, the intensity of spectra increases from 2.5 (bottom), 5, 10, 15, 20, 30, 40, to 50 mg L^{-1} (top) of Re(IV).

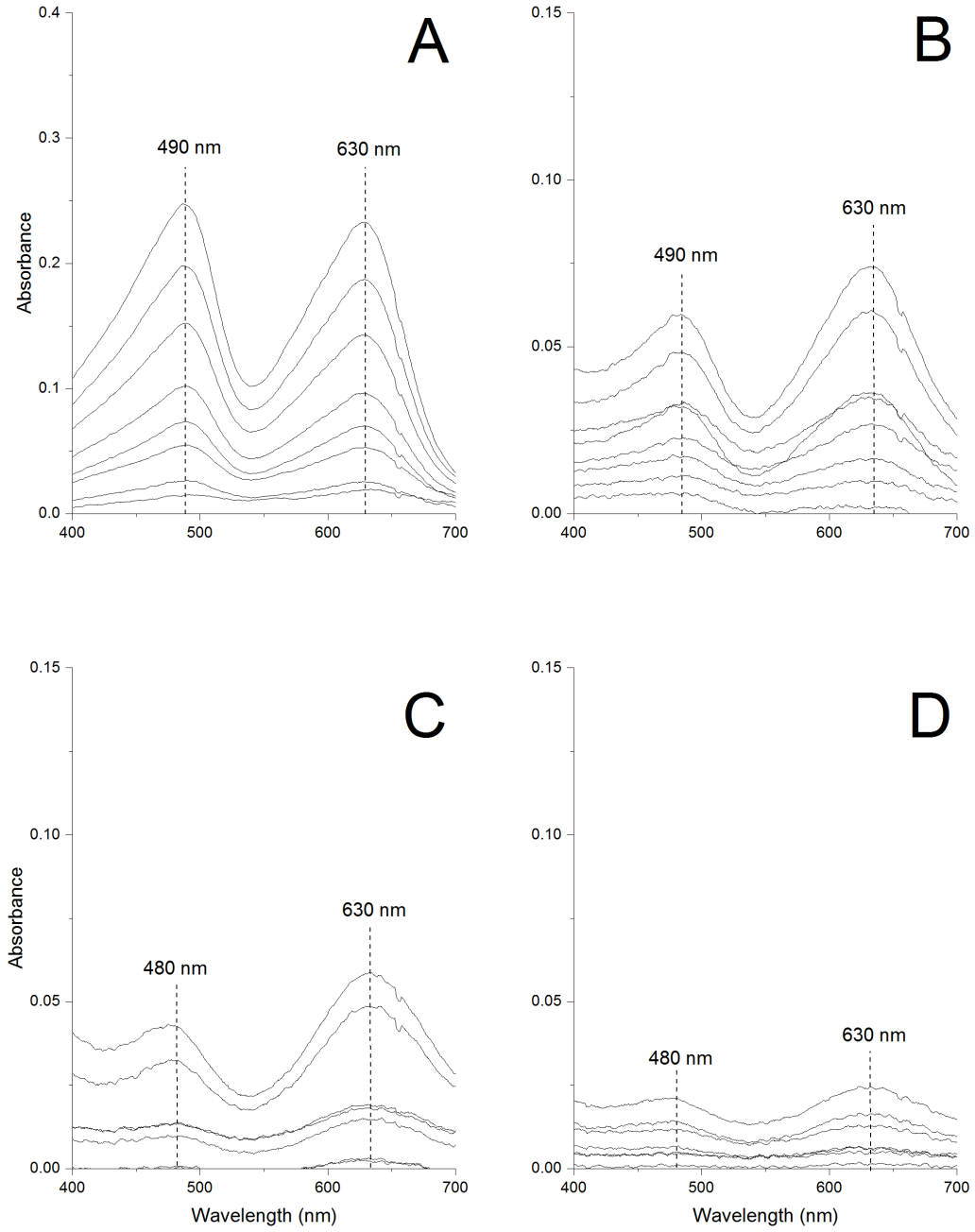

Figure 2.9: Absorbance spectra of Re(IV)-methyl-2-pyridyl ketoxime complex (Thompson et al., 1964) in $NaNO_3$ background solutions, A) 0.001M, B) 0.01M, C) 0.05M and D) 0.1M. In each figure, the intensity of spectra increases from 2.5 (bottom), 5, 10, 15, 20, 30, 40, to 50 mg L^{-1} (top) of Re(IV).

2.8 Tables

Table 2.1: Results of linear regression analysis of spectra absorbance of Re(IV)-pyridyl thiourea complex at 405 nm in Mili-Q, $NaNO_3$ and $NaHCO_3$ media. ε (L mg^{-1} cm^{-1}): absorptivity. All samples were assessed at [Re]: 2.5 - 50 mg L^{-1} except for the samples in 0.5M $NaNO_3$. 2.5 mg L^{-1} Re standard was not detected in 0.5M $NaNO_3$.

Reaction Condition	**ε (L mg^{-1} cm^{-1})**	**R^2**
Mili-Q	0.0051	0.9943
0.001M $NaHCO_3$	0.0053	0.9930
0.01M $NaHCO_3$	0.0054	0.9985
0.05M $NaHCO_3$	0.0057	0.9976
0.1M $NaHCO_3$	0.0053	0.9933
0.5M $NaHCO_3$	0.0055	0.9966
0.001M $NaNO_3$	0.0049	0.9977
0.01M $NaNO_3$	0.0038	0.9978
0.05M $NaNO_3$	0.0032	0.9988
0.1 M $NaNO_3$	0.0031	0.9951
0.5 M $NaNO_3$	0.0027	0.9897

Table 2.2: Results of linear regression analysis at absorbance maxima in Mili-Q water and $NaNO_3$, $NaHCO_3$ media. ε (L mg^{-1} cm^{-1}): absorptivity. The regression analysis was performed at the limited detection range noted in the table.

Reaction Condition	Detection range (mg L^{-1} Re)	Absorbance maxima (nm)	ε (L mg^{-1} cm^{-1})	R^2
Mili-Q water	2.5 – 10	403	0.005	0.9737
Mili-Q water	15 – 30	398	0.0055	0.9932
0.001M $NaHCO_3$	10 – 20	400	0.0051	0.9734
0.001M $NaHCO_3$	30 – 50	390	0.0058	0.9991
0.01M $NaHCO_3$	10 – 20	400	0.0055	0.9956
0.01M $NaHCO_3$	30 – 50	390	0.0059	0.9989
0.05M $NaHCO_3$	10 – 20	400	0.0057	0.9990
0.05M $NaHCO_3$	30 – 50	390	0.0061	0.9998
0.1M $NaHCO_3$	10 – 20	400	0.0056	0.9947
0.1M $NaHCO_3$	30 – 50	390	0.0057	0.9901
0.5M $NaHCO_3$	10 – 20	400	0.0056	0.9896
0.5M $NaHCO_3$	30 – 50	390	0.0058	0.9996
0.001M $NaNO_3$	10 – 20	400	0.0052	0.9942
0.001M $NaNO_3$	30 – 50	385	0.0053	0.9990
0.01M $NaNO_3$	10 – 20	400	0.0037	0.9816
0.01M $NaNO_3$	30 – 50	385	0.0038	0.9994
0.05M $NaNO_3$	10 – 20	380	0.0035	0.9902
0.05M $NaNO_3$	30 – 50	370	0.0042	0.9995
0.1M $NaNO_3$	2.5 – 50	360	0.0058	0.9967
0.5M $NaNO_3$	2.5 – 50	355	0.0097	0.9407

Table 2.3: Results of linear regression analysis of spectra absorbance of Re(IV)- methyl-2-pyridyl ketoxime complex at 490 and 630nm in Mili-Q water and $NaNO_3$, $NaHCO_3$ media. ε (L mg^{-1} cm^{-1}): absorptivity. BD: below detection.

		Wavelength				
		490 nm		630 nm		
Reaction Condition	**Detection range (mg L^{-1})**	**ε (L mg^{-1} cm^{-1})**	**R^2**	**Detection range (mg L^{-1})**	**ε (L mg^{-1} cm^{-1})**	**R^2**
Mili-Q Water	2.5 – 50	0.0063	0.9969	2.5 – 50	0.0055	0.9968
0.001M $NaHCO_3$	2.5 – 50	0.0063	0.9988	2.5 – 50	0.0057	0.9985
0.01M $NaHCO_3$	2.5 – 50	0.0065	0.9968	2.5 – 50	0.0056	0.9969
0.05M $NaHCO_3$	2.5 – 50	0.0063	0.9990	2.5 – 50	0.0057	0.9989
0.1M $NaHCO_3$	2.5 – 50	0.0063	0.9985	2.5 – 50	0.0056	0.9983
0.5M $NaHCO_3$	2.5 – 50	0.0064	0.9990	2.5 – 50	0.0057	0.9965
0.001M $NaNO_3$	2.5 – 50	0.0050	0.9984	2.5 – 50	0.0047	0.9974
0.01M $NaNO_3$	BD	-	-	-	-	-
0.05M $NaNO_3$	BD	-	-	-	-	-
0.1M $NaNO_3$	BD	-	-	-	-	-
0.5M $NaNO_3$	BD	-	-	-	-	-

2.9 References

Agnihotri P., Deb M., Thakur M. and Mishra R. (1998) Spectrophotometric determination of rhenium(IV) with thiocyanate, TX-100 and N,N '-diphenylbenzamidine. *J. Chin. Chem. Soc.* **45,** 401-406.

Almond P. M., Stefanko D. B. and Langton C. A. (2013) Effect of Oxidation on Chromium Leaching and Redox Capacity of Slag-Containing Waste Forms. Cementitious Barriers Partnership, CBP-TR-2013-02.

Altshuller A. P. and Wartburg A. F. (1960) Ultraviolet Determination of Nitrogen Dioxide as Nitrite Ion. *Anal. Chem.* **32,** 174-177.

Bard A. J., Parsons R. and Jordan J. (1985) *Standard potentials in aqueous solution.* Marcel Dekker, New York.

Burns D. T. and Tungkananuruk N. (1988) Spectrophotometric determination of rhenium as perrhenate after extraction of its brilliant green ion-pair with microcrystalline benzophenone. *Anal. Chim. Acta* **204,** 359-363.

Burns D., El-Shahawi M., Kerrigan M. and Smyth P. (1996) Spectrophotometric determination of rhenium as perrhenate by extraction with amiloride hydrochloride. *Anal. Chim. Acta* **322,** 107-109.

Collos Y., Mornet F., Sciandra A., Waser N., Larson A. and Harrison P. J. (1999) An optical method for the rapid measurement of micromolar concentrations of nitrate in marine phytoplankton cultures. *J. Appl. Phycol.* **11,** 179-184.

Dutta G. and Sur B. (1986) Spectrophotometric Determination of Rhenium using 2-Pyridyl Thiourea. *Mikrochim. Acta* **1,** 359-369.

Finch M., Hydes D., Clayson C., Weigl B., Dakin J. and Gwilliam P. (1998) A low power ultra violet spectrophotometer for measurement of nitrate in seawater: introduction, calibration and initial sea trials. *Anal. Chim. Acta* **377,** 167-177.

Gangopadhyay S., Gangopadyay P. and Shome S. (1976) Spectrophotometric Determination of Rhenium with Thiobenzhydrazide. *Anal. Chim. Acta* **83,** 409-413.

Hindman J. C. and Wehner P. (1953) Electrolytic Reduction of Perrhenate. I. Studies in Perchloric, Ethanesulfonic, Trifluoroacetic and Hydrochloric Acids. *J. Am. Chem. Soc.* **75,** 2869-2872.

Kassner J. L., Ting S. and Grove E. L. (1961) Spectrophotometric determination of rhenium with 4-methylnioxime1. *Talanta* **7,** 269-275.

Kliegman J.M and Barnes R.K. (1972) The Reaction of Nitrous Acid with Oximes. *J. Org. Chem.* **37,** 4223-4225.

Kormosh Z. and Bazel Y. (1999) Extraction of oxyanions with basic polymethine dyes from aqueous and aqueous-organic solutions: Extraction-photometric determination of rhenium(VII) and tungsten(VI). *J. Anal. Chem.* **54,** 607-611.

Lukens W. W., McKeown D. A., Buechele A. C., Muller I. S., Shuh D. K. and Pegg I. L. (2007) Dissimilar behavior of technetium and rhenium in borosilicate waste glass as determined by X-ray absorption spectroscopy. *Chem. Mat.* **19,** 559-566.

Maun E. K. and Davidson N. (1950) Investigations in the Chemistry of Rhenium. I. Oxidation States IV, V and VII. *J. Am. Chem. Soc.* **72,** 254-2260.

Meloche V., Martin R. and Webb W. (1957) Spectrophotometric Determination of Rhenium with Alpha-Furildioxime. *Anal. Chem.* **29,** 527-529.

Nechamkin H. (1968) *The Chemistry of the Elements.* McGraw-Hill, New York.

Plieth W. J. (1973) In *Encyclopedia of the Electrochemistry of the Elements* (ed. A. J. Bard). Marcel Dekker, New York.

Poineau F., Fattahi M., Den Auwer C., Hennig C. and Grambow B. (2006) Speciation of technetium and rhenium complexes by in situ XAS-electrochemistry. *Radiochim. Acta* **94,** 283-289.

Savariar C. P. and Hariharan T. R. (1975) An extraction-spectrophotometric method for the determination of rhenium using mixed ligands. *Mikrochim. Acta* **63,** 477-483.

Schwochau K. (2000) *Technetium: chemistry and radiopharmaceutical applications*. Wiley-VCH, Weinheim.

Sommer L. (1989) *Analytical Absorption Spectrophotometry in the Visible and Ultraviolet: The Principles.* Elsevier, Amsterdam.

Spalding R. and Exner M. (1993) Occurrence of Nitrate in Groundwater - a Review. *J. Environ. Qual.* **22,** 392-402.

Stumm W. and Morgan J. J. (1996) *Aquatic Chemistry: Chemical Equilibria and Rates in Natural Waters.* Wiley, New York.

Thompson R. J., Gore R. H. and Trusell F. (1964) Methyl-2-pyridyl ketoxime as a colorimetric reagent for rhenium. *Anal. Chim. Acta* **31,** 590-594.

Wahi A. and Kakkar L. (1997) Microdetermination of rhenium with Rhodamine-B and thiocyanate using ascorbic acid as the reductant. *Anal. Sci.* **13,** 657-659.

Wetters J. H. and Uglum K. L. (1970) Direct spectrophotometric simultaneous determination of nitrite and nitrate in the ultraviolet. *Anal. Chem.* **42,** 335-340

Chapter 3: Kinetics and Extent of Re(VII) Sorption to Zerovalent Iron

3.1 Abstract

Technetium(Tc)-99 is one of major risk drivers in low level radioactive liquid waste at the U.S. Department of Energy sites. Cementitious waste technology (CWT) has been considered for immobilizing pertechnetate, $Tc(VII)O_4^-$, as Tc(IV) oxides and sulfides with the use of reducing agents like slag. In this study, zero valent iron (ZVI) was evaluated as a potential reducing agent in CWT as a function of pH (8.2-10.2) and [nitrate] (0-0.1M) using perrhenate, $Re(VII)O_4^-$, as an analogue for $Tc(VII)O_4^-$. Batch $Re(VII)O_4^-$ sorption experiments showed that the sorption decreased with increasing pH from 7 to 12. Although the extent of ReO_4^- sorption decreased with increasing pH and [nitrate], pseudo 2nd order kinetic rates increased with increasing [nitrate] which was attributed to co-adsorption of NH_4^+ (i.e., a reaction product of reduced nitrate by ZVI), facilitating electrostatic attraction towards ReO_4^- under alkaline conditions. Overall the results show that Re(VII) can be immobilized in ZVI as much as 20% at pH 10.2 and 0.1M nitrate. Considering the thermodynamically favorable reduction of Tc(VII) over Re(VII), ZVI might offer an alternative to slag for promoting the immobilization of Tc(VII) by reductive precipitation within CWT.

3.2 Introduction

Radioactive waste is of growing concern in the United States and around the world. Environmental contamination of radionuclides is a serious issue with use of nuclear power sources. Technetium-99 (^{99}Tc) ($t_{1/2}$: 2.1 x 10^5 yr) is produced from induced fission of ^{235}U. A common nuclear reactor operating at normal conditions can produce approximately 1 MBq of total Tc radioactivity per year (Schwochau, 2000). Prior to being banned, nuclear weapon testing also released ^{99}Tc into the environment. Levels of ^{99}Tc from these types of tests are estimated between 100 and 160 TBq across the world (Schulte and Scoppa, 1987; Yoshihara, 1996).

Currently, the United States Department of Energy (DOE) is considering the immobilization of ^{99}Tc in low level radioactive waste (LLW) using cement technology. Since pertechnetate ($Tc(VII)O_4^-$) is highly mobile in the environment, reduction of Tc(VII) to Tc(IV) is the key to form insoluble Tc(IV) oxide and sulfide species.

At the Savannah River site (SRS), saltstone formulation (slag, fly ash, and portland cement) has been demonstrated since 1990 (Kaplan and Hang, 2007). Blast furnace slag (BFS)

and fly ash are major ingredients in the saltstone cement formulation that creates a reducing environment within the cement in order to immobilize ^{99}Tc. At the Hanford site, a cast stone project is currently considered as a future project.

The critical process/element of CWT technology is to have an effective electron donor to reduce Tc(VII) to Tc(IV). In alkaline conditions, sulfide-rich slag present in CWT solutions can rapidly oxidize to sulfate in solutions containing $Ca(OH)_2$ and NaOH, therefore possibly compromising its reductive capacity in such environments (Roy, 2009). Many researchers are currently seeking better electron donors to effectively reduce Tc(VII).

Zero-Valent Iron (ZVI), a byproduct of the reduction of ferric chloride or ferrous sulfate with borohydride and also is a byproduct of the steel manufacturing industry, which may have economic feasibility for to use as a reducing agent on larger scales. It has been shown to effectively reduce various metals such as chromium, lead, uranium, and molybdenum (Cantrell et al., 1995; Ponder et al., 2000). Such contaminants are commonly reduced to an insoluble form using ZVI. Hazardous non-metal compounds such as trichloroethylene have also been treated similarly with ZVI (Xin et al., 2015). This suggests that ZVI could be a more effective reducing agent in CWT.

Several researchers have also reported the reduction of rhenium (Re), a chemical analogue of Tc, by ZVI (Ding et al., 2013; Liu et al., 2013).Their work shows Re reduction by ZVI most rapid at pH 8, and can be increased by raising temperature, can also increase the reaction rate, and that the reaction product in both studies was precipitated $ReO_{2(s)}$. Based on the thermodynamic calculation below, reduction of Tc(VII) by ZVI at pH 10 is thermodynamically more favorable than the reduction of Re(VII).

$$2ReO_4^- + H_2O + 2Fe(0) \rightarrow 2ReO_2 + 2OH^- + Fe_2O_3$$

$$\Delta G = \Delta G_{products} - \Delta G_{reactants} = \mathbf{-526.194\ kJ/mol}$$

$$2TcO_4^- + H_2O + 2Fe(0) \rightarrow 2TcO_2 + 2OH^- + Fe_2O_3$$

$$\Delta G = \Delta G_{products} - \Delta G_{reactants} = \mathbf{-1104.394\ kJ/mol}$$

In the case of cement immobilization technology, the system is highly alkaline. The reduction of $Tc(VII)O_4^-$ at high pH will be further suppressed. Unfortunately, there is little information on the reduction capacity of ZVI in cementitious materials. The objective of this study is to evaluate the reduction of Re(VII) using synthetic ZVI in simulated environmental conditions (e.g., pH > 7, presence of bicarbonate and nitrate anions) of low-level radioactive waste (LLW) (Almond et al. 2012). Comparing ΔG of Tc reduction at alkaline pH, Re(VII) reduction is less favorable than that of Tc(VII). Therefore, if the experiment shows Re(VII) reduction by ZVI, it suggests that Tc(VII) will be more effectively reduced under the same reaction conditions. Results gained from this study should give insight to the practicality of using ZVI to create a reducing environment for Tc within CWFs and document any interferences caused by bicarbonate and nitrate present in LLW.

3.3 Methods

ZVI Synthesis

All chemicals were ACS-grade, and mili-Q water was boiled and purged with N_2 prior to the use. The synthesis of ZVI was performed using a modified method described by Ponder and co-workers (Ponder et al., 2000). Instead of ferrous sulfate, ferric chloride was used to eliminate sulfide contamination during ZVI synthesis. 16 g of $FeCl_3 \cdot 6H_2O$ was dissolved in 150 mL of degassed mili-Q water, and then $NaBH_4$ was added incrementally in 1.6 times the molar amount of $FeCl_3 \cdot 6H_2O$. $NaBH_4$ was slowly added allowing H_2 gas formed to subside between increments. The solution mixture was then shaken for approximately 20 min. and then filtered via vacuum filtration using 0.45 µm Millipore type HA gridded membrane filter paper (Millipore, Billerica, MA). After filtering, the remaining solids were washed liberally with 15 mL of degassed Mili-Q water and then washed with 100% ethanol. Washing with freshly synthesized ZVI with degassed Mili-Q prior to redox experiments has been a common practice in previous studies (Garcell et al., 1998; Hwang et al., 2015; Mallet et al., 2013; Moore and Young, 2005; Rennert and Mansfeldt, 2002). This fresh ZVI was immediately used for each redox kinetic experiment. Moisture content of fresh ZVI was measured before and after vacuum drying ZVI, and $[Fe]_{total}$ was used to express the mass of fresh ZVI used in each experiment. The washing process was also important to remove residual chloride anions. Although chloride anions do not strongly sorb on the ZVI surfaces since Point of Zero Charge (PZC) of ZVI is approximately 7 (Suponik et al., 2015). At neutral pH, there should be no strong attraction

between Cl^- and the ZVI surface. The washing process assures negligible chloride contamination in our experimental system. Our preliminary experiment showed that washing with degassed mili-Q water at neutral pH was sufficient to remove residual chloride anions from ZVI.

Point of Zero Charge

The Point of Zero Charge (PZC) of the ZVI particles was measured using the method described by Ferris and Jepson (1975). Measurements were carried out in 30 mL sample bottles containing a ZVI suspension of 5 g/L. A pH range of 5 to 12 was provided by incremental additions of 1.8 M HCl or 0.6 M NaOH. An ammonium chloride (NH_4Cl) stock solution was added to each the bottles to achieve a final [NH_4^+] and [Cl^-] concentration of 0.5 mM. Sorption of both NH_4^+ and Cl^- were analyzed and the PZC of the ZVI particles was determined at a crossover point. The reaction vessels were shaken on an end-over shaker at 18 rpm for 24 hr. The ZVI suspensions were passed through 0.2 µm polyvinylidene fluoride (PVDF) filters, and then aliquots were analyzed for [chloride] by ion chromatography using an ICS-1600 model (Dionex, Sunnyvale, CA). Ammonium concentration was determined using a QuikChem FIA+ 8000 Series flow injection analysis method (Hach Company, Loveland, CO).

$Re(VII)O_4^-$ sorption in ZVI as a function of pH

Ao as to simulate mixing conditions of current CWT, the pseudo-equilibrium sorption experiments of ReO_4^- in ZVI were conducted as a function of pH (4 to 12) (ZVI: solution ratio: 2.5 g/L, an initial [ReO_4^-]: 0.27 mM, and 0.3M NaCl electrolyte) under the atmospheric condition ($pCO_2 = 10^{-3.4}$ atm). This was to simulate the mixing condition of the current CWT. The 0.3M electrolyte concentration was used to maintain similar ionic strength conditions required in the kinetic studies. For example, the pH 8.3 kinetic test conditions required high amounts of $NaHCO_3^-$ (0.2M) to provide adequate buffering and high $NaNO_3$ concentrations (0.1M). The freshly synthesized ZVI was added to the NaCl solution to allow pH equilibration for several hours and then the suspensions were spiked with the ReO_4^- stock solution. The reaction vessels were shaken on an end-over shaker at 18 rpm overnight, followed by pH measurement. ZVI suspensions were then filtered through 0.2 µm PVDF filters, and aliquots were analyzed spectrophotometrically for ReO_4^- concentration using the spectrophotometric method (Dutta and Sur, 1986; Lenell and Arai, 2016).

Batch Kinetic Method

Batch kinetic tests of Re reduction by ZVI were carried out in 30-mL bottles with an initial Re concentration of 0.27 mM and a 10 g/L ZVI concentration. Different carbonate buffer solutions for pH values of 8.3, 9.2, and 10.2 were introduced to an empty vessel containing 0.3 g of synthesized ZVI particles and then sonified in a water bath. Sample trials were also prepared with increasing amounts of NO_3^- at 0.001M, 0.01M, and 0.1M in order to evaluate effects on Re reduction. Ionic strength of all samples was adjusted to 0.3M by addition of NaCl. This was done to ensure a more uniform distance of the diffuse double layer between ZVI particles amongst all of the tested reaction conditions in order to give proper comparison between pH and nitrate factors. Duplicate bottles were sacrificially sampled at 10 min, 30 min, 1, 3, 6, 12, and 24 hours by pipetting a 5 mL aliquot from the bottle. The aliquot samples were then filtered through a 0.2 µm PVDF syringe filter. The resulting filtrate was completely clear, having no visible traces of the solid Fe. Samples were then analyzed for aqueous Re using the spectrophotometric analysis method (Dutta and Sur, 1986; Lenell and Arai, 2016). The kinetic data were modeled using the pseudo-second order model presented by Ho and McKay (1998). This was done using the following equation:

$$\frac{t}{q_t} = \frac{1}{kq_c{}^2} + \frac{1}{q_c}t \qquad \text{(Eq. 1)}$$

where q_t is the amount of Re sorbed onto ZVI at a unit time in mg/g. The q_c term is the modeled amount of Re sorbed onto ZVI at equilibrium, and is determined in equation (1) by plotting t/q_t vs. t where the slope of the fit line is equal to $1/q_c$. The rate constant k (g/mg hr) is determined from equation (1) by the same linear plot and using the intercept value to solve for k.

Kinetic data for the experiments were also fitted with a pseudo-first order reaction model, as in the study by Zhou et al., (2016). Equation (2) was used below:

$$\ln(q_c - q_t) = \ln q_c - kt \qquad \text{(Eq. 2)}$$

Where q_t and q_c are similar to the variables described above which is the sorption of Re onto ZVI. The rate constant for this equation was determined by observing the slope of the best fit line for the plot of $\ln(q_c - q_t)$ vs time. Underlying assumptions involved in these two pseudo-order rate models is that the concentration of iron remains relatively constant in comparison to perrhenate because it is supplied in great excess. Ho and McKay (1999) also report that an assumption is made in their model that the rate is limited by exchange of electrons between sorbent and sorbate, which is applicable to this system as well.

Dissolved Iron Measurements

Ferrous iron and total Fe analysis were performed for kinetic samples by using the 1,10-phenanthroline method (Stucki, 1981). The original procedure was followed except for the solid digestion steps. Unless otherwise specified, all reagents (10% (w/w) 1,10-phenanthroline, 5% boric acid (H_3BO_3), and 1% sodium citrate ($Na_3C_6H_5O_7$)) were prepared using ACS-grade chemicals and mili-Q water. Ferrous ion standards were prepared by dissolving ammonium iron(II) sulfate $(NH_4)_2Fe(SO_4)_2 \cdot 6H_2O$ in water. To assess [Fe(II)] in kinetic samples, all analytical procedures were performed in darkness under red light to prevent photochemical reduction of Fe(III) to Fe(II) after addition of phenanthroline. To each 2-mL kinetic sample, 1 mL of 10% (w/w) 1,10-phenanthroline, 2 mL of 5% (w/w) boric acid (H_3BO_3) and 10 mL of 1% sodium citrate dihydrate were added. Samples were then analyzed at 510 nm using a Cary 5 spectrophotometer (Agilent Technologies, Santa Clara, CA). For $[Fe]_{total}$ analysis, the same samples were exposed to fluorescent light for approximately 1 hr to induce photochemical reduction of Fe(III) to Fe(II). After the light exposure, the samples were then re-measured at 510 nm to estimate $[Fe]_{total}$.

3.4 Results and Discussion

Point of Zero charge Characterization of ZVI

Figure 3.1 shows Cl^- and NH_4^+ sorption onto the synthesized ZVI particles. Based on the trend lines, the cross over point is the PZC, which is at about 8.4. Other PZC values for ZVI have been previously reported at around pH 7.7 (Arancibia-miranda et al., 2014) also pH 8.1-8.3 (Sun

et al., 2006). Therefore, the value obtained in this study is consistent with those in the literature values.

Effect of pH on ReO_4^- Sorption by ZVI

Figure 3.2 shows the results of ReO_4^- sorption in ZVI after 24 hrs. The Re(VI) sorption was highest at near neutral pH. And the sorption decreases with decreasing pH from near neutral pH to 3. At low pH, the activity of protons is high. Protons readily accept electrons from ZVI, resulting in the formation of $H_2(g)$, which was observed during the experiments. This reaction, in turn, would cause less of the electron donor, ZVI, to be available for $Re(VII)O_4^-$. The production of H_2 gas was observed during the experiments. The reduction of H^+ by ZVI at acidic pH is shown below (Liu et al., 2013). Gibbs free energy of the oxidation of ZVI by protons is negative, indicating that the reaction is spontaneous (Benjamim, 2015).

$$Fe^0 + 2H^+ \rightarrow Fe^{2+} + H_{2\,(g)} \qquad \Delta G = -78.87\,\frac{kJ}{mol}$$

It is also apparent that ReO_4^- sorption was inhibited in alkaline conditions. The reduction in Re sorption is attributed to 1) auto oxidation of ZVI and 2) surface charge property. The ZVI surface becomes more passive towards Re(VII) reduction due to the formation of Fe-hydroxides at the surface (Chen et al., 2001; Tian et al., 2009; Yang and Lee, 2005). Yoon and co-workers state that when dissolved iron species are formed during oxidation reactions of ZVI in water (Yoon et al., 2011). Two oxidation reactions of ZVI are suggested by Furukawa and co-workers (2000).

$$Fe^0 + \frac{1}{2}O_2 + H_2O \rightarrow Fe^{2+} + 2OH^-$$

and

$$Fe^0 + 2H_2O \rightarrow Fe^{2+} + H_2 + 2OH^-$$

The newly dissolved ferrous species can further react with OH^- that is present in solution to form ferrous hydroxide species, which can then further oxidize to form $Fe^{III, II}$ (oxyhydr)oxide compounds such as magnetite, lepidocrocite, ferrihydrite, and goethite, in turn pacifying the ZVI surface towards further reduction reactions. (Furukawa et al., 2002; Li et al., 2014; Yoon et al., 2011). Perrhenate reduction can also be inhibited due to a higher negative surface charge of the ZVI particles in alkaline solution. Since the ReO_4^- anions are not attracted to the negatively charged surface under these conditions (pH > PZC), electron transfer reactions are suppressed (Liu et al., 2013; Yuan et al., 2010).

The Extent of Re(VII) Sorption in ZVI

Figures 3.3, 3.4 and 3.5 show the removal of Re(VII) from the solution that is expressed in a ratio of $[Re]_i$:$[Re]_0$ as a function of time, pH and $[NO_3]$. $[Re]_i$ is the concentration of Re(VII) at given time, $[Re]_0$ is the initial Re[(VII) concentration. Table 3.1 summarizes the results of % Re(VII) sorbed in ZVI after 24 hrs. It is important to note that [nitrate] was greater than [Re(VII)] except for the control systems (i.e., no nitrate).

At all pH values tested, the addition of nitrate decreases the total amount of Re(VII) sorbed. After 24hrs, [Re(VII)] remaining in the solution increases with increasing $[NO_3^-]$. The same trend is observed in at all pH values. Nitrate is a competitive electron acceptor for ZVI, since nitrate is more favorably reduced by ZVI than perrhenate. Thus lowering the reduction capacity of ZVI for Re(VII) when nitrate is added. Thermodynamic calculations of the NO_3^- and Re(VII) reduction by ZVI are shown below at standard state condition.

$$4Fe(0) + NO_3^- + 7H_2O \rightarrow 4Fe(II) + NH_4^+ + 10OH^-$$

$$\Delta G^O = -620\ kJ$$ (Kielemoes et al., 2000)

$$ReO_4^- + 4H^+ + Fe(0) \rightarrow ReO_2 + 2H_2O + Fe(III)$$

$$\Delta G^O = -136\ kJ$$ (Bard et al., 1985; Ebbing and Wrighton 1993)

Several researchers documented NH_4^+ as the product of nitrate reduction when nitrate was reacted with ZVI (Ahn et al., 2008; Cho et al., 2015; Rodriguez-Maroto et al., 2009). The reaction is further inhibited as the surface of ZVI gets oxidized by Re(VII) and nitrate, and thus preventing the reduction of Re(VII) at the surface.

The effect of pH was also observed under the respective [NO_3^-]. At pH 8.3, 9.2 and 10.2, Re(VII) sorption decreased from 91% to 39%, 88.35% to 35.50%, 29.34% to 9.70%, respectively. The highest amount of Re(VII) sorption was observed at pH 8.2. Comparing to the control systems without any nitrate, little Re(VII) sorption occurs at pH 10.2. Although the effect of pH was small from 8.3 to 9.2, it is clear that the reaction extent decreases with increasing pH. At lower pH (e.g., 8.2 < PZC) without nitrate, surface charge density is less negative than that at higher pH (10.2 > PZC). This is a preferred condition for Re(VII) to approach the ZVI surfaces. One can expect more reduction of Re(VII) to occur at pH 8.2 than at pH 10.2. As Re(VII) gets reduced, more Fe(0) gets oxidized. This will increase solubility of Fe(II) as well as Fe(III) as long as the system is undersaturated with respect to Fe(II)/Fe(III) oxyhydroxides at given pH. Figures 3.6-3.8 show the release of Fe(III) for the kinetic samples. Most of dissolved Fe(II) was below the detection limit of the phenanthroline method (<0.19 μM); the majority of dissolved iron shown in the figures is present as Fe(III). At pH 8.3, [Fe(III)] generally peaked after several hours, and gradually decreases with increasing time (Fig 3.6). The same kinetic trend in the Fe(III) release was observed at pH 9.2 and 10.2 (Figs 3.7 and 3.8). At a fixed [NO_3^-] in Figs 3.6-3.8, the quantity of [Fe(III)] decreases with increasing pH. In the pH 8.3 system, [Fe(III)] remained less than 0.08mM (Fig 3.8). In the pH 9.2 system, the release of Fe(III) is no more than 0.025mM (Fig 3.7). At pH 10.2, the amount of Fe(III) release further decreases to <0.02mM in all conditions (Fig 3.8). The Fe dissolution data support the pH-dependent Re(VII) sorption data. A decrease in the extent of Re(VI) sorption at alkaline pH can also be described by the formation of reaction products from auto oxidation of ZVI. At high pH, auto oxidation of the ZVI surface is also expected, forming iron hydroxide coatings (Li et al., 2014). This iron hydroxide layer can suppress the electron transfer reactions between ZVI and Re(VII), which in turn lowers the reductive capacity of the ZVI particles at alkaline pH (Liu et al., 2013).

Effects of Nitrate Concentration on Kinetic Rates

As described in the method section, pseudo 1st and 2nd order models were used to estimate the rate of Re(VII) sorption per unit mass of solid ZVI surface in the solution. Linear fits for these models are displayed in figures 3.9 – 3.14, in the four panels of each figure, 1st and 2nd order fits are displayed in the right and left column respectively, for each tested reaction condition. A summary of rate constants along with the goodness of fit values are shown in Table 3.1. When the 1st order model was used, a poor goodness of fit (<0.95) was observed in the samples at pH 10.2, and in some samples in the presence of nitrate (e.g., pH 8.3, 0.001M NaNO3). Overall, the pseudo 2nd order model had yielded in a better goodness of fit (>0.97) for most of reaction conditions. For this reason, the following discussion is based on the kinetic rate in the pseudo 2nd order model for all conditions.

Increasing [NO_3^-] within each pH value results in an increase in kinetic rate, the rate was increased from 0.023 g mg^{-1} hr^{-1} to 1.429 g mg^{-1} hr^{-1} at pH 8.2, from 0.03 to 1.8099 at pH 9.2 and from 0.1154 to 3.3371 g mg^{-1} hr^{-1} at pH 10.2, respectively. This process is explained by the charge neutrality effect by the adsorption of NH_4^+ on the ZVI surfaces. Ammonium ions were generated during the reduction of nitrate by ZVI according to the reaction mentioned earlier in the sorption extent discussion.

$$4Fe(0) + NO_3^- + 7H_2O \rightarrow 4Fe(II) + NH_4^+ + 10OH^- \qquad \text{(Kielemoes et al., 2000)}$$

The release of [NH_4^+] in each kinetic system is shown in Figures 3.15 -3.17. Adding more nitrate has yielded in greater production of ammonium. Figure 3.1 clearly showed that ammonium adsorption was enhanced at alkaline pH values. The adsorption of ammonium on the ZVI surface makes the surface charge of ZVI less negative. This in turn, causes an electrostatic attraction of perrhenate anions to the NH_4^+ adsorbed ZVI surfaces. Figure 3.18 explains how NH_4^+ can facilitate attraction of perrhenate in these alkaline conditions.

3.5 Conclusion

The results of this study provide insight regarding the use of ZVI particles in cementitious waste technology to immobilize ^{99}Tc. Using ReO_4^- as a chemical surrogate of $Tc(VII)O_4^-$, effects of reaction conditions (i.e., pH and nitrate concentration) on the ReO_4^-

sorption by synthetic ZVI particles were investigated. Over a broad pH range from pH 4-12, ReO_4^- showed highest sorption over a 24 hr period at near neutral pH conditions. Sorption onto ZVI was found to decrease under both acidic and alkaline conditions. More surface corrosion of ZVI is expected to occur within acidic conditions due to surface oxidation by H^+, preventing further donation of electrons to $Re(VII)O_4^-$. In alkaline conditions, the formation of Fe-hydroxides at the surface likely causes the ZVI particles to become more passified, potentially diminishing ZVI surface reactivity towards $Re(VII)O_4^-$. The surface charge of ZVI also becomes increasingly more negative in alkaline solution, causing less charge attraction between perrhenate anions and the ZVI surfaces. Overall, these factors contribute to impede the electron transfer reactions under extreme pH conditions. Kinetic experiments exhibited less reaction extent both with increasing pH from 8.3 to 10.2 and $[NO_3^-]$ concentration from 0M to 0.1M. Interestingly, the kinetic rate increased with increasing $[NO_3^-]$. Addition of $[NO_3^-]$ facilitates the production of NH_4^+, which adsorbs strongly to the ZVI surface under alkaline conditions. This charge neutrality facilitates an electrostatic attraction of perrhenate anions, resulting in an increase of the rate of Re(VII) reduction.

Although the Re(VII) sorption was limited at high pH and high nitrate conditions, the reduction of Re(VII) occurred. Because reduction is more thermodynamically favorable for Tc(VII) than Re(VII), the results of this study have positive implications for improving the current cement waste form formulation such as saltstone. Further work should be done in evaluating effectiveness of ZVI in these chemical systems. Furthermore, if one can suppress the auto oxidation of ZVI with chemical coatings, it may be possible to incorporate the ZVI as a potential reducing agent in highly alkaline LLW solutions. Some studies have involved the use of starches during the synthesis process (Ding et al., 2013; Dong and Lo, 2013; He and Zhao, 2005). This improves particle stability by making them less susceptible to surface oxidation, and prevents agglomeration of particles in solution in order to maintain higher surface area, thereby improving overall treatment effectiveness (Saleh et al., 2007). Additionally, some methods of treatment have looked into incorporating additional electron donors, specifically sulfide, in order to improve the reducing capacity of ZVI towards TcO_4^-, and to facilitate formation of insoluble Tc(IV)sulfide species in addition to Tc(IV) oxides (Fan et al., 2013).

3.6 Figures

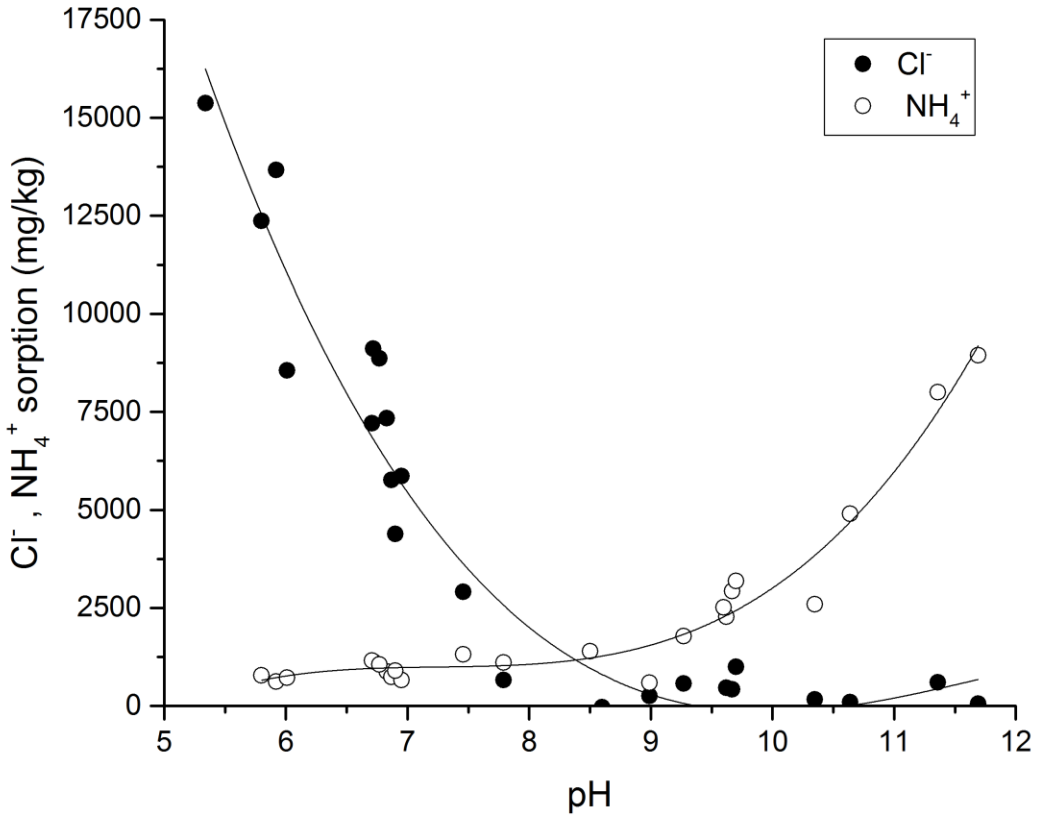

Figure 3.1: Chloride and ammonium adsorption in ZVI as a function of pH (suspension density: a 5 g/L and initial $[NH_4Cl]_i$ = 5 mM). A cross over point of two trend lines indicates Point of Zero Charge: ~8.4.

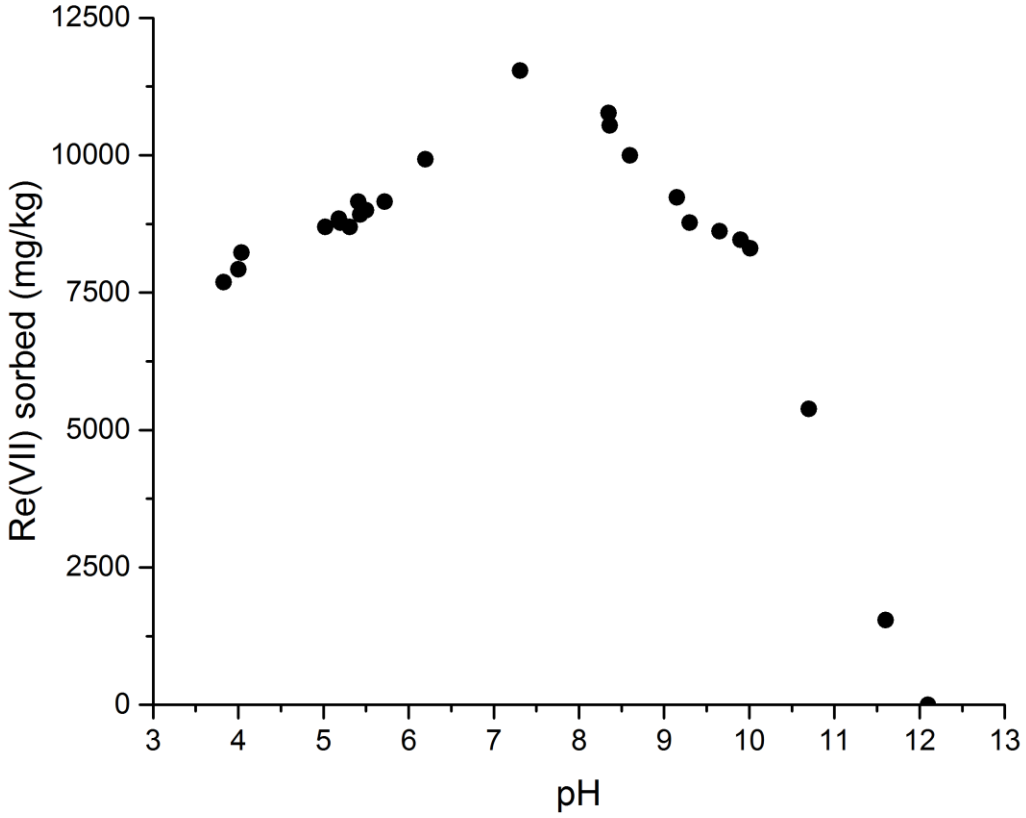

Figure 3.2: Re(VII) sorption in ZVI as a function of pH (suspension density: 2.5 g/L, reaction time: 24 hrs, background electrolyte: 0.3M NaCl, and initial [Re(VII)]:0.27 mM).

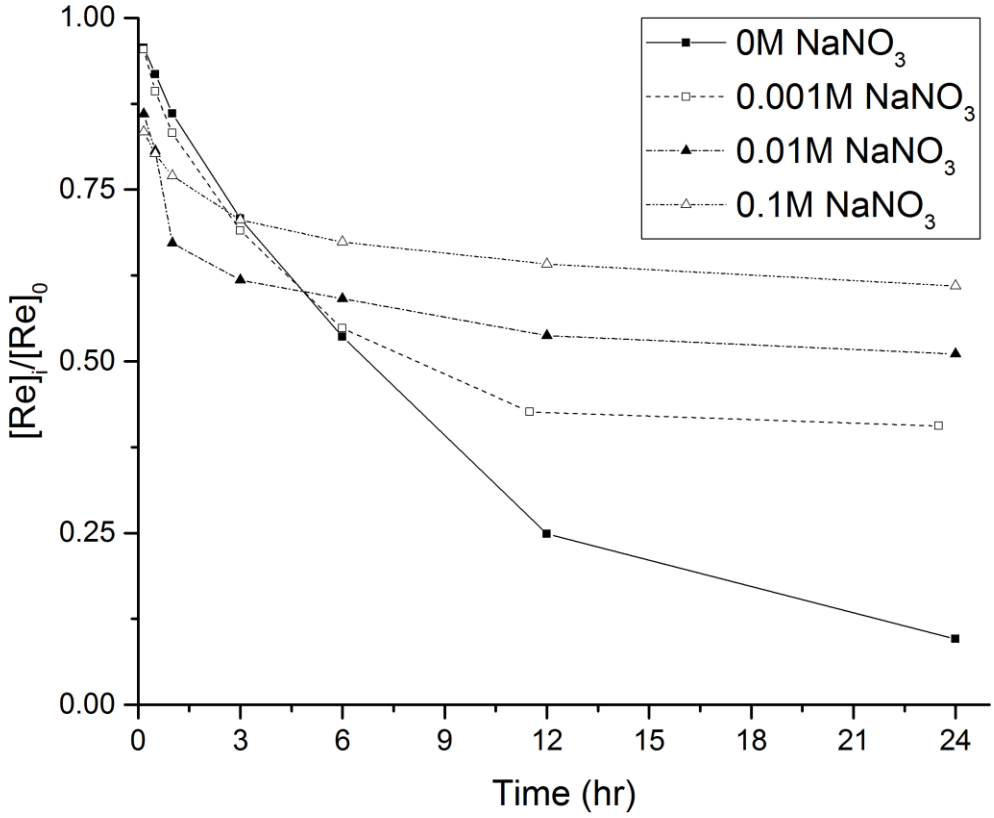

Figure 3.3: The extent of Re(VII) sorption in ZVI at pH 8.3 at [$NaNO_3$]: 0-0.1M. $[Re]_i/[Re]_0$ is plotted against time in hrs.

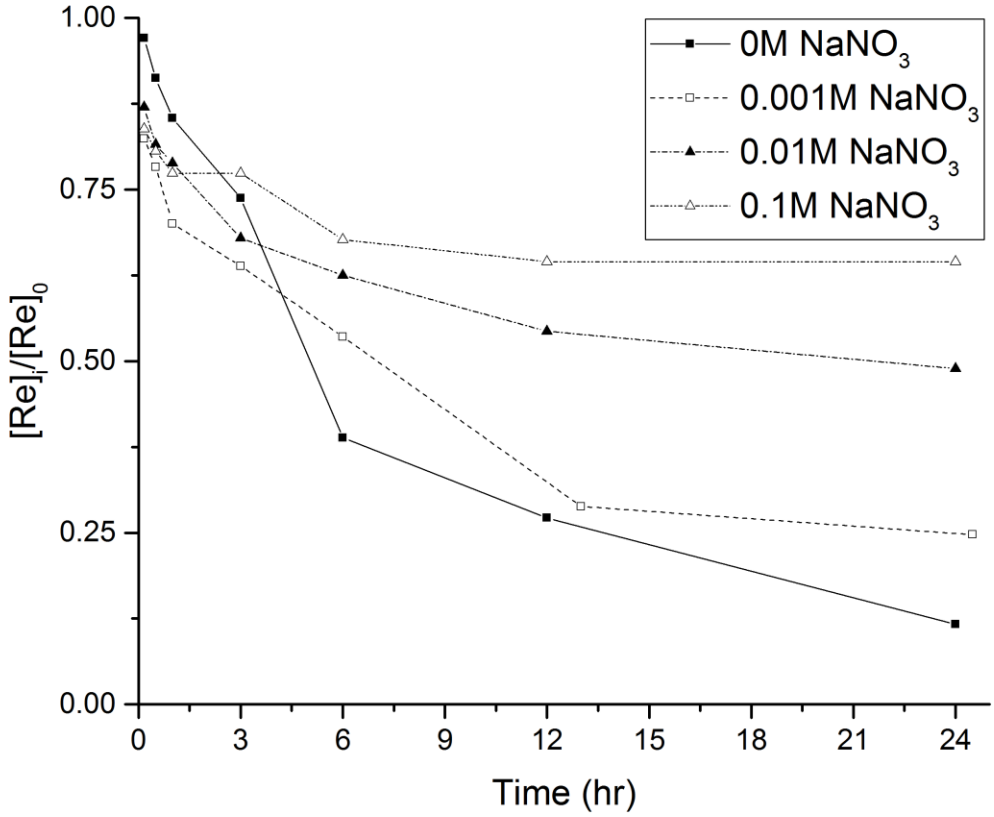

Figure 3.4: The extent of Re(VII) sorption in ZVI at pH 9.2 at [$NaNO_3$]: 0-0.1M. $[Re]_i/[Re]_0$ is plotted against time in hrs.

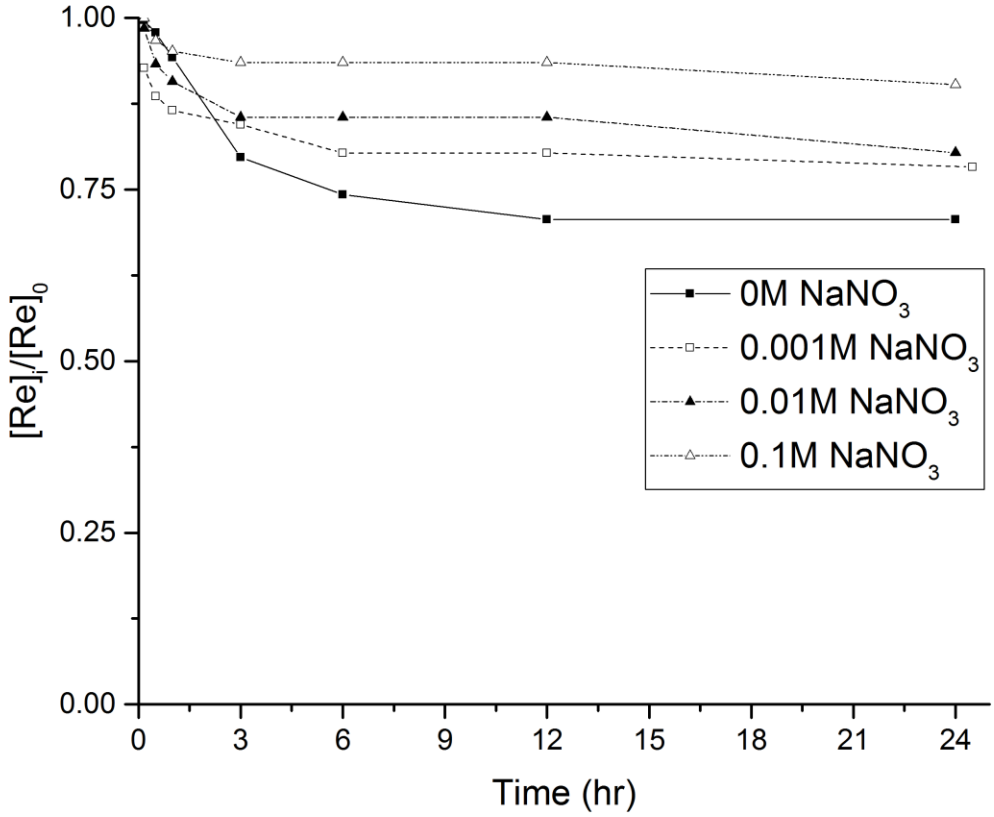

Figure 3.5: The extent of Re(VII) sorption in ZVI at pH 10.2 at [$NaNO_3$]: 0-0.1M. $[Re]_i/[Re]_0$ is plotted against time in hrs.

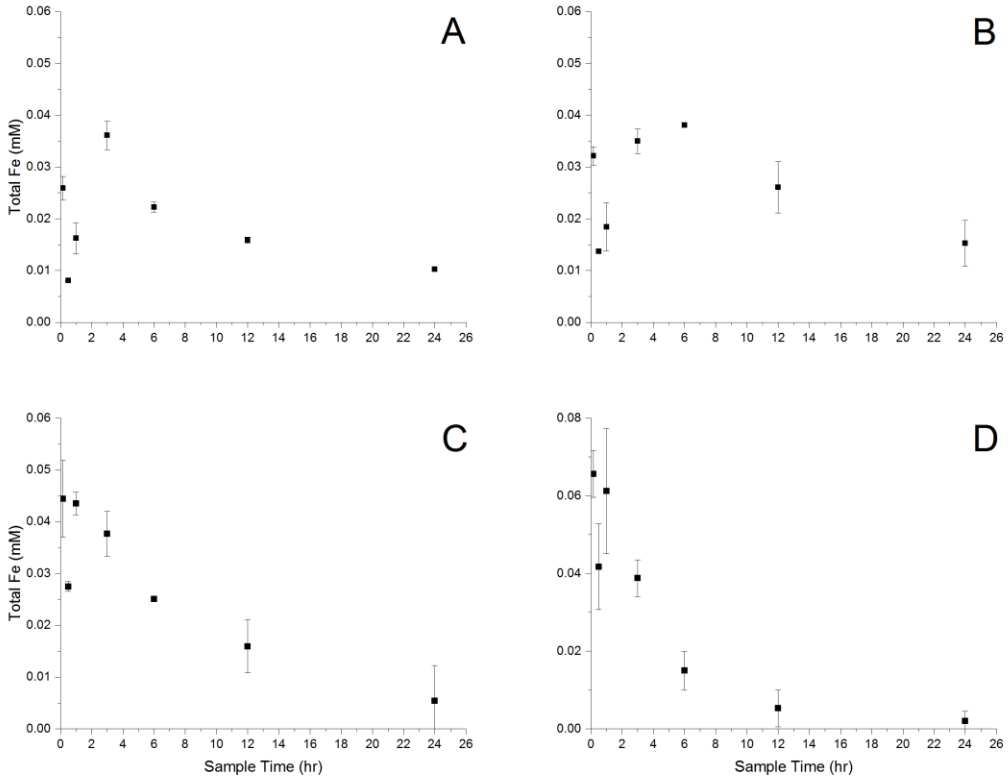

Figure 3.6: Release of Fe(III) during the Re(VII) sorption in ZVI at pH 8.3 shown in Fig 3.3. A: 0M $NaNO_3$, B: 0.001M $NaNO_3$, C: 0.01M $NaNO_3$, and D: 0.1M $NaNO_3$.

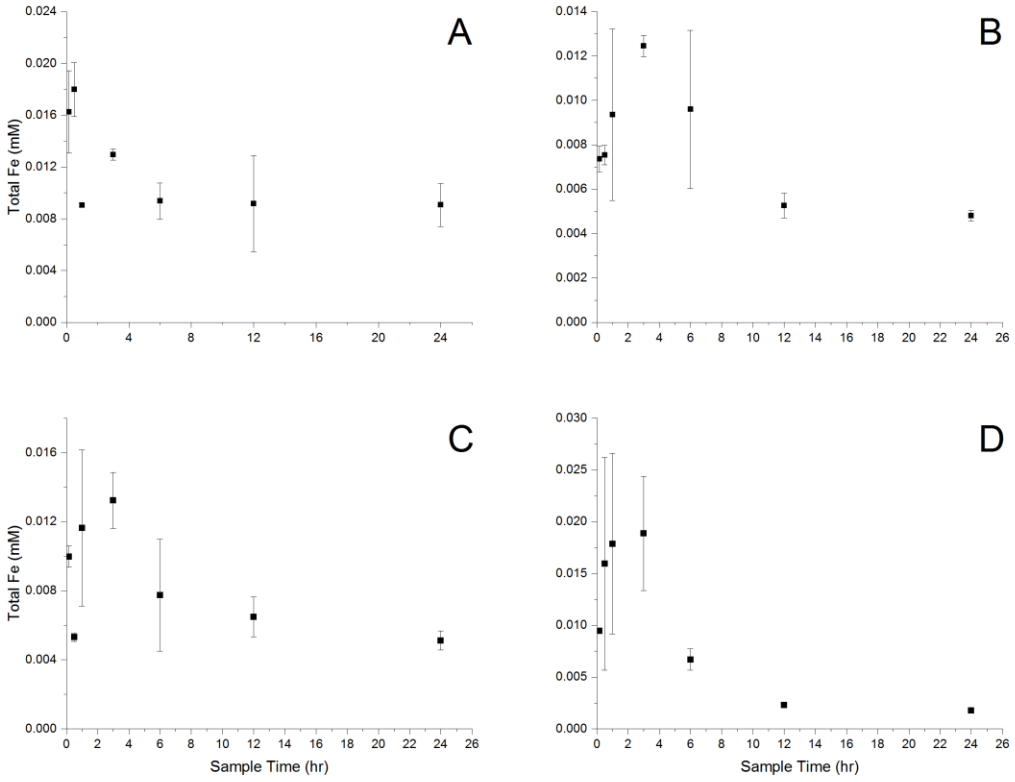

Figure 3.7: Release of Fe(III) during the Re(VII) sorption in ZVI at pH 9.2 shown in Fig 3.4. A: 0M $NaNO_3$, B: 0.001M $NaNO_3$, C: 0.01M $NaNO_3$, and D: 0.1M $NaNO_3$.

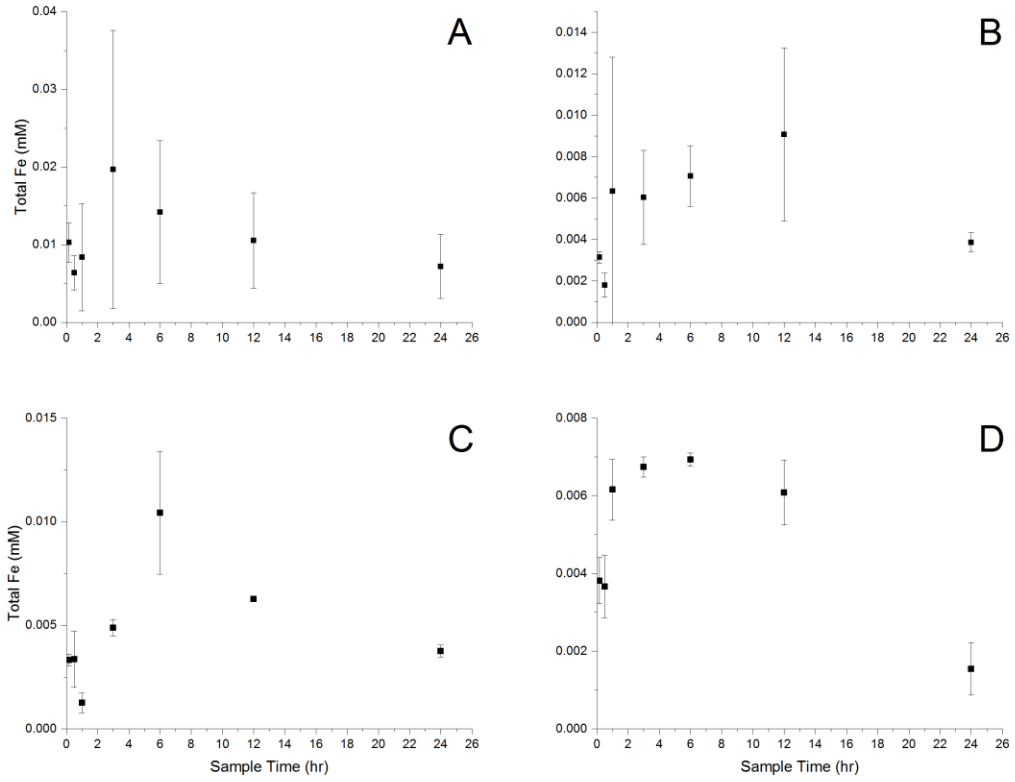

Figure 3.8: Release of Fe(III) during the Re(VII) sorption in ZVI at pH 10.2 shown in Fig 3.5. A: 0M $NaNO_3$, B: 0.001M $NaNO_3$, C: 0.01M $NaNO_3$, and D: 0.1M $NaNO_3$.

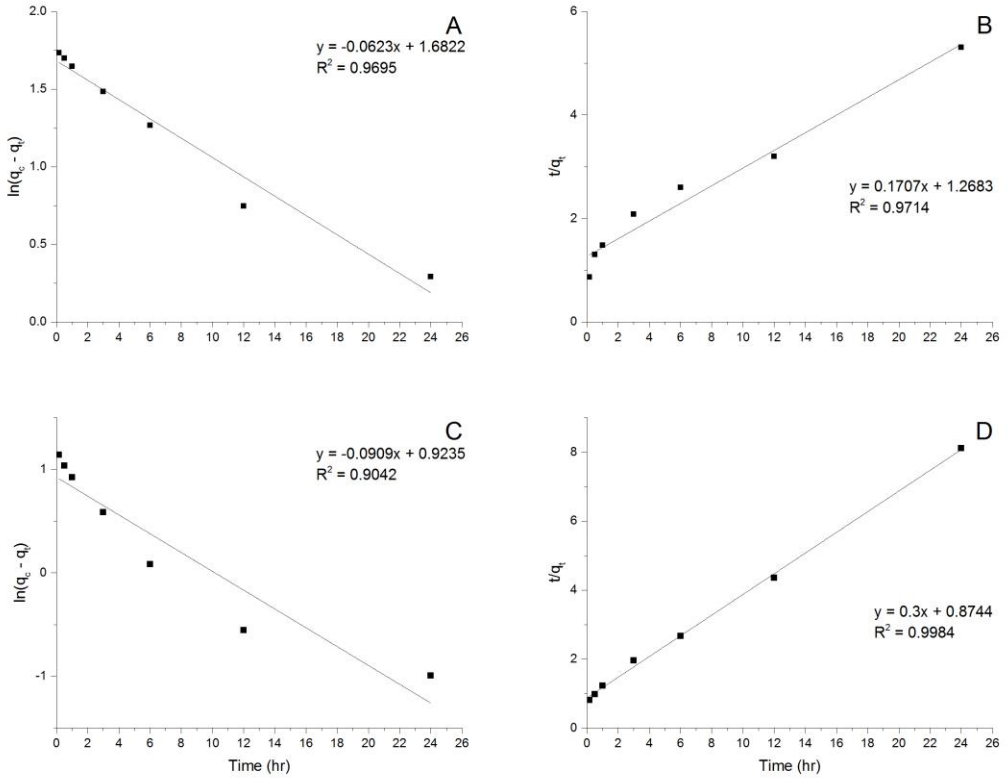

Figure 3.9: Results of kinetic model fit in the Re(VII) sorption data in ZVI at pH 8.3 shown in Fig 3.3. Pseudo 1st order model fit for the 0M $NaNO_3$ and 0.001M $NaNO_3$ is shown in A and C, respectively. Pseudo 2nd order kinetic model fit for the 0M $NaNO_3$ and 0.001M $NaNO_3$ is shown in B and D, respectively.

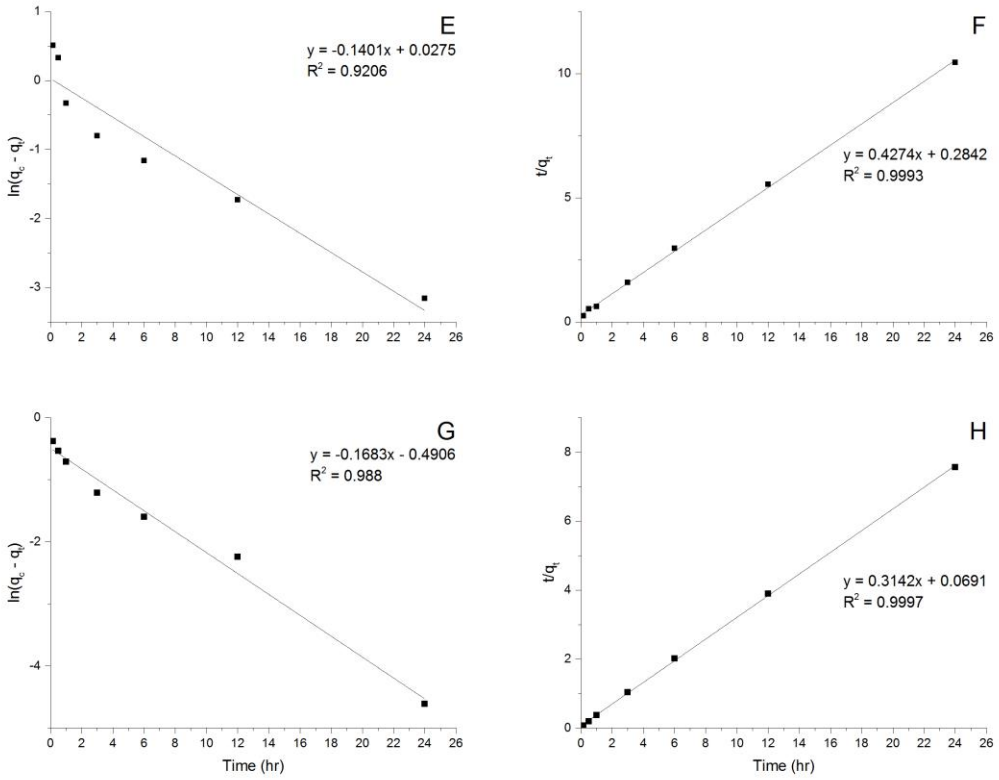

Figure 3.10: Results of kinetic model fit in the Re(VII) sorption data in ZVI at pH 8.3 shown in Fig 3.3. Pseudo 1st order model fit for the 0.01M $NaNO_3$ and 0.1M $NaNO_3$ is shown in A and C, respectively. Pseudo 2nd order kinetic model fit for the 0.01M $NaNO_3$ and 0.1M $NaNO_3$ is shown in B and D, respectively.

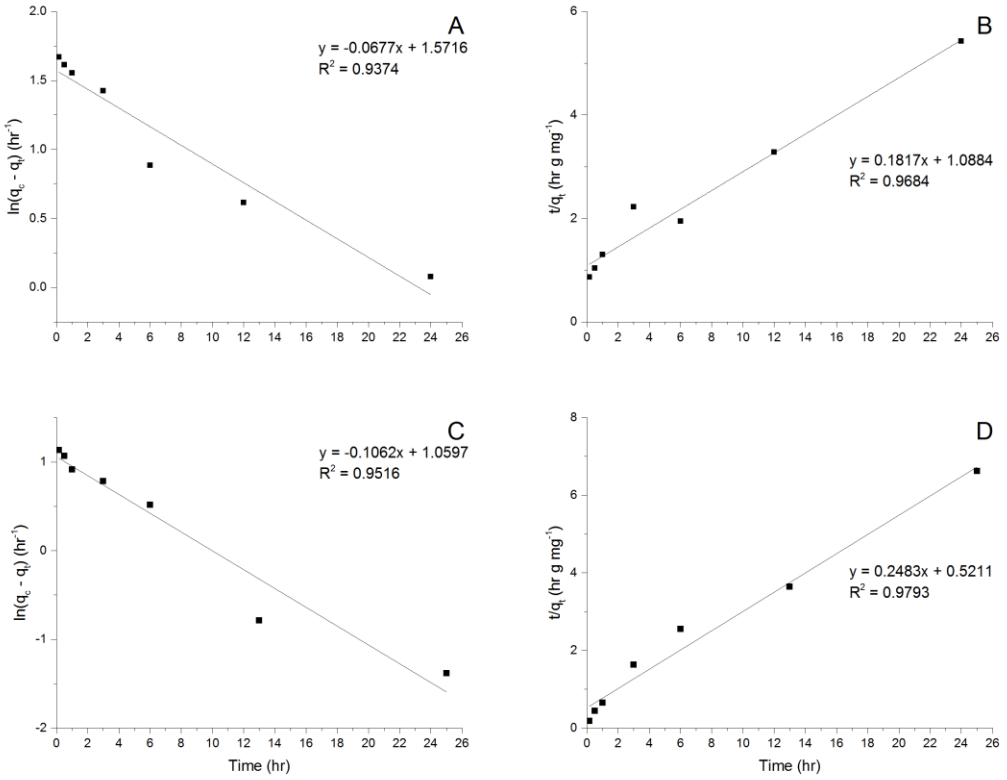

Figure 3.11: Results of kinetic model fit in the Re(VII) sorption data in ZVI at pH 9.2 shown in Fig 3.4. Pseudo 1st order model fit for the 0M $NaNO_3$ and 0.001M $NaNO_3$ is shown in A and C, respectively. Pseudo 2nd order kinetic model fit for the 0M $NaNO_3$ and 0.001M $NaNO_3$ is shown in B and D, respectively.

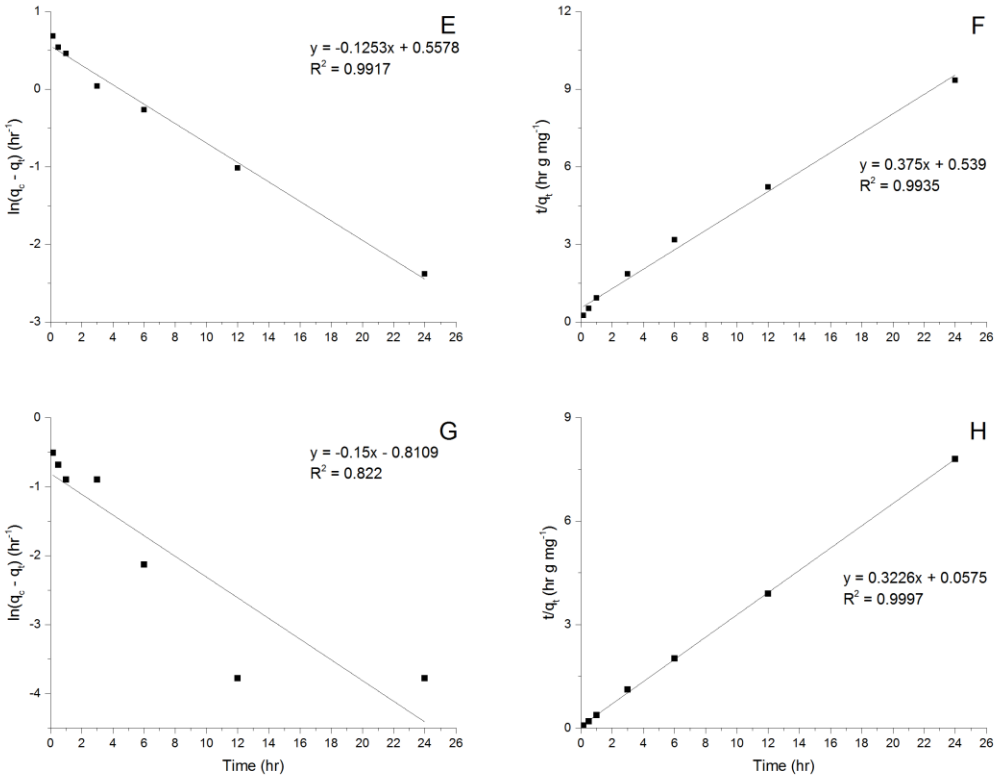

Figure 3.12: Results of kinetic model fit in the Re(VII) sorption data in ZVI at pH 9.2 shown in Fig 3.4. Pseudo 1st order model fit for the 0.01M $NaNO_3$ and 0.1M $NaNO_3$ is shown in A and C, respectively. Pseudo 2nd order kinetic model fit for the 0.01M $NaNO_3$ and 0.1M $NaNO_3$ is shown in B and D, respectively.

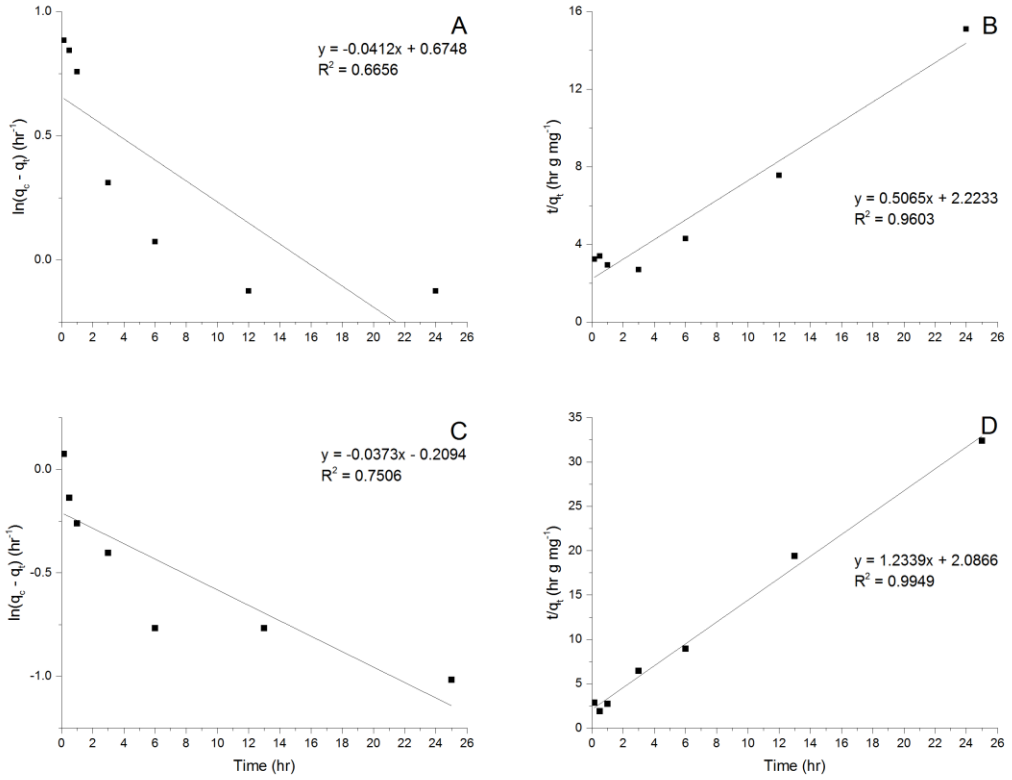

Figure 3.13: Results of kinetic model fit in the Re(VII) sorption data in ZVI at pH 10.2 shown in Fig 3.5. Pseudo 1st order model fit for the 0M $NaNO_3$ and 0.001M $NaNO_3$ is shown in A and C, respectively. Pseudo 2nd order kinetic model fit for the 0M $NaNO_3$ and 0.001M $NaNO_3$ is shown in B and D, respectively.

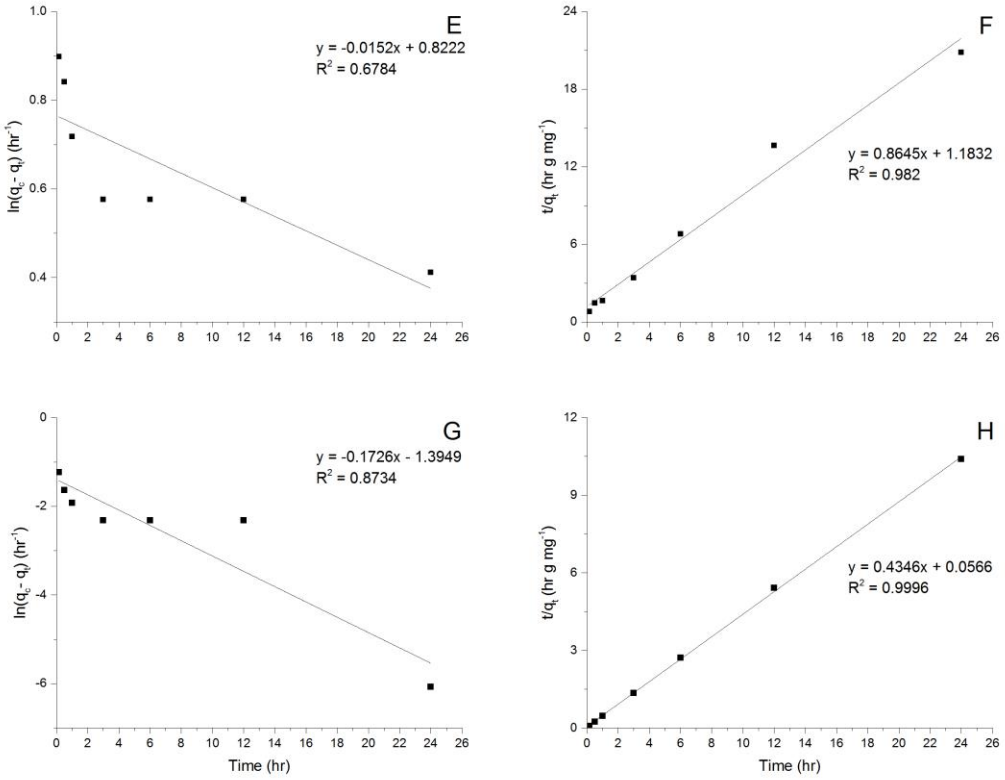

Figure 3.14: Results of kinetic model fit in the Re(VII) sorption data in ZVI at pH 10.2 shown in Fig 3.5. Pseudo 1st order model fit for the 0.01M $NaNO_3$ and 0.1M $NaNO_3$ is shown in A and C, respectively. Pseudo 2nd order kinetic model fit for the 0.01M $NaNO_3$ and 0.1M $NaNO_3$ is shown in B and D, respectively.

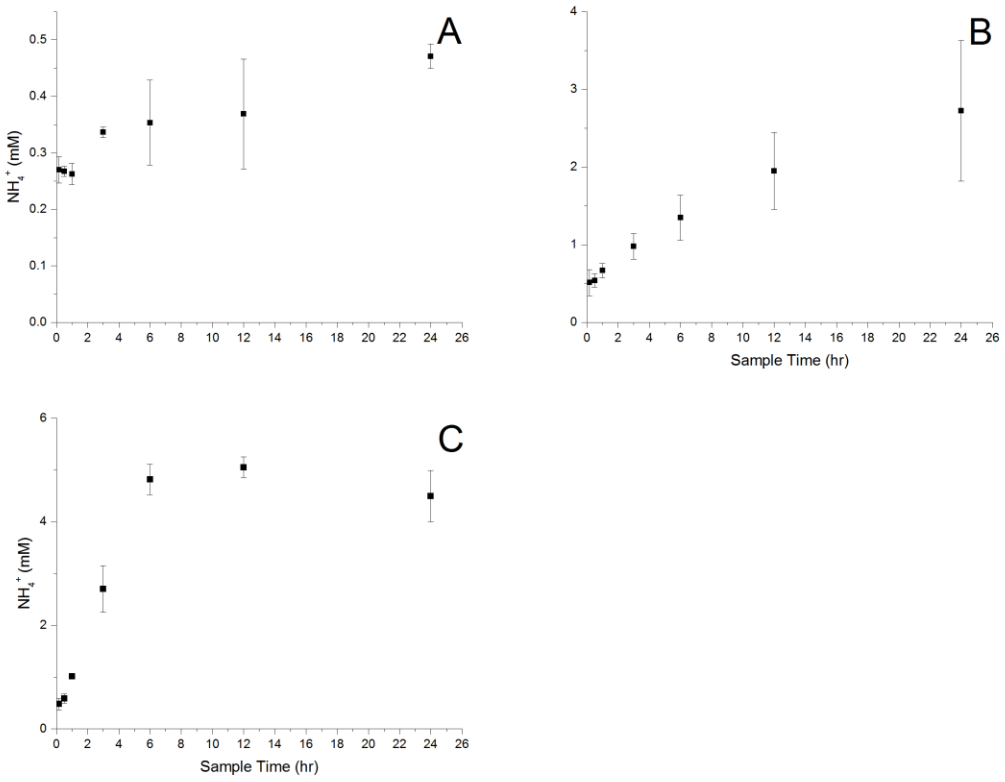

Figure 3.15: Production of ammonium in pH 8.3 kinetic samples (Fig 3.3) as a function of initial [NO_3^-]. A: 0.001M, B: 0.01M, and C: 0.1M.

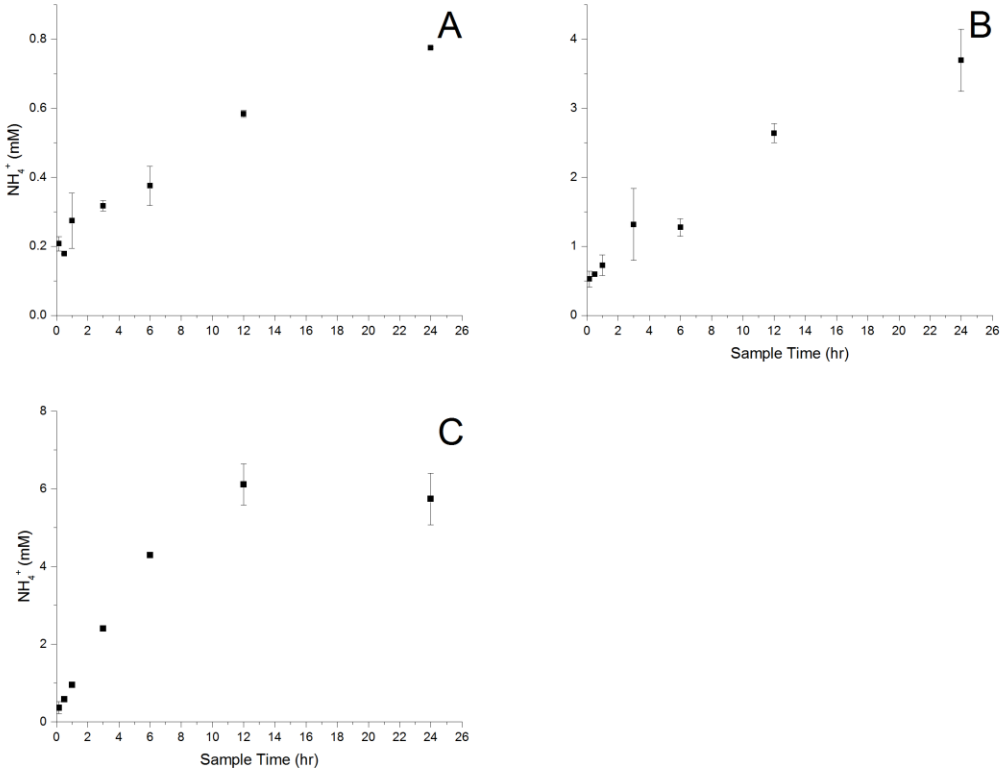

Figure 3.16: Production of ammonium in pH 9.2 kinetic samples (Fig 3.4) as a function of initial [NO_3^-]: A: 0.001M, B: 0.01M, and C: 0.1M.

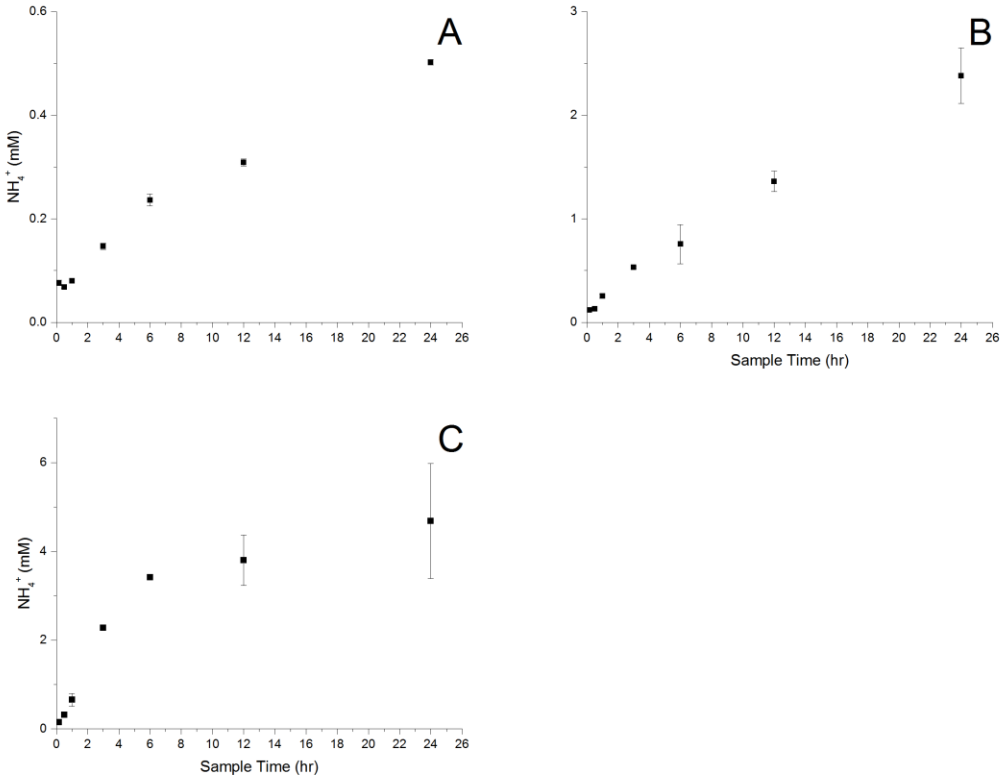

Figure 3.17: Production of ammonium in pH 10.2 kinetic samples (Fig 3.5) as a function of initial $[NO_3^-]$: A: 0.001M, B: 0.01M, and C: 0.1M.

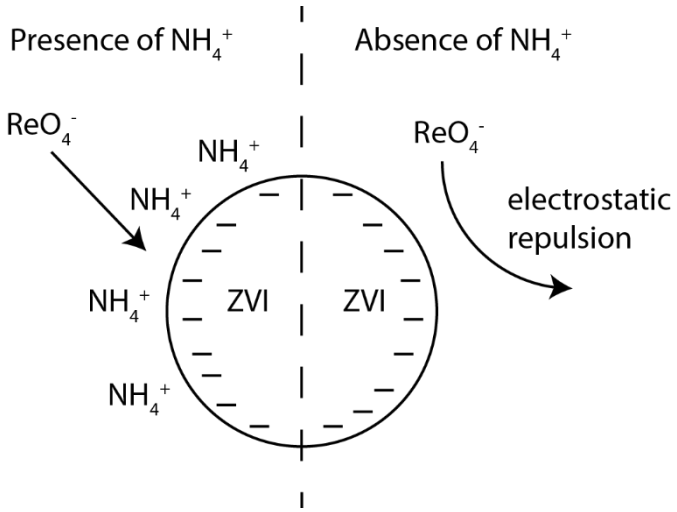

Figure 3.18: Ammonium adsorption enhanced ReO_4^- adsorption in ZVI under alkaline conditions (modified from Cho et al., 2015).

Table 3.1: Summary of reaction extents and pseudo 1st and 2nd order rates for Re(VII) sorption in ZVI as a function of reaction conditions. Values in parenthesis indicate goodness of fit from kinetic model fit.

Reaction conditions	**Kinetic rate**			
	% Re(VII) sorbed after 24 hours	**Pseudo 1st order model, hr^{-1}**		**Pseudo 2nd order model, g mg^{-1} hr^{-1}**	
pH 8.3, 0 M $NaNO_3$	90.44	0.0623	(0.9695)	0.023	(0.9714)
pH 8.3, 0.001 M $NaNO_3$	59.41	0.0909	(0.9042)	0.10293	(0.9984)
pH 8.3, 0.01 M $NaNO_3$	48.93	0.1401	(0.9206)	0.643	(0.9993)
pH 8.3, 0.1 M $NaNO_3$	39.05	0.1683	(0.988)	1.429	(0.9997)
pH 9.2, 0 M $NaNO_3$	88.35	0.0677	(0.9374)	0.030	(0.9684)
pH 9.2, 0.001 M $NaNO_3$	75.28	0.1062	(0.9516)	0.1183	(0.9793)
pH 9.2, 0.01 M $NaNO_3$	51.07	0.1253	(0.9917)	0.261	(0.9935)
pH 9.2, 0.1 M $NaNO_3$	35.50	0.15	(0.822)	1.8099	(0.9997)
pH 10.2, 0 M $NaNO_3$	29.34	0.0423	(0.6656)	0.1154	(0.9603)
pH 10.2, 0.001 M $NaNO_3$	19.91	0.0373	(0.7506)	0.7297	(0.9949)
pH 10.2, 0.01 M $NaNO_3$	19.65	0.0162	(0.6784)	0.6315	(0.982)
pH 10.2, 0.1 M $NaNO_3$	9.70	0.1726	(0.8734)	3.3371	(0.9996)

3.8 References

Ahn S. C., Oh S. and Cha D.K. (2008) Enhanced reduction of nitrate by zero-valent iron at elevated temperatures. *J. Hazard. Mater.* **156,** 17-22.

Almond P., Kaplan D., Langton C., Stefanko D., Spencer W., Hatfield A. and Arai Y. (2012) Method evaluation and field sample measurements for the rate of movement of the oxidation front in saltstone. Savannah River National Laboratory. SRNL-STI-2012-00468.

Arancibia-miranda N., Baltazar S. E., García A., Romero A. H., Rubio M. A., and Altbir, D. (2014) Lead removal by nano-scale zero valent iron : Surface analysis and pH effect. *Mater. Res. Bull.* **59,** 341–348.

Bard A. J., Parsons R. and Jordan J. (1985) *Standard potentials in aqueous solution.* Marcel Dekker, New York.

Benjamin, M. (2015) *Water Chemistry*. Waveland Press, Inc. Long Grove, IL.

Cantrell K.J., Kaplan D.I., Wietsma T.W. (1995) Zero-valent iron for the in situ remediation of selected metals in groundwater. *J. Hazard. Mater.* **42,** 201-212.

Chen J., Al-Abed S.R., Ryan J.A. and Li Z. (2001) Effects of pH on dechlorination of trichloroethylene by zero-valent iron. *J. Hazard. Mater.* **B83,** 243-254.

Cho D., Song H., Schwartz F. W., Kim B. and Jeon B. (2015) The role of magnetite nanoparticles in the reduction of nitrate in groundwater by zero-valent iron. *Chemosphere* **125,** 41-49.

Ding Q., Qian T., Yang F., Liu H., Wang L., Zhao D. and Zhang M. (2013) Kinetics of reductive immobilization of rhenium in soil and groundwater using zero valent iron nanoparticles. *Environ. Eng. Sci.* **30,** 713-718.

Dong H. and Lo I.M.C. (2013) Influence of humic acid on the colloidal stability of surface-modified nano zero-valent iron. *Water Res.* **47,** 419-427.

Dutta G. and Sur B. (1986) Spectrophotometric Determination of Rhenium Using 2-Pyridyl Thiourea. *Mikrochim. Acta.* **1,** 359-369.

Ebbing D. D. and Wrighton M.S. (1993) *General Chemistry, 4th edition.* Houghton Mifflin, Boston.

Fan D., Anitori R.P., Tebo B.M., Tratnyek P.G., Pacheco J.S.L., Kukkadapu R.K., Engelhard M.H., Bowden M.E., Koverik L., Arey B.W. (2013) Reductive Sequestration of Pertechnetate ($^{99}TcO_4^-$) by Nano Zerovalent Iron (nZVI) Transformed by Abiotic Sulfide. *Environ. Sci. Technol.* **47,** 5302-5310.

Ferris A.P. and Jepson W.B (1975) The Exchange Capacities of Kaolinite and the Preparation of Homoionic Clays. *J. Colloid Interface Sci.* **51,** 245-259.

Furukawa Y., Kim J., Watkins J. and Wilkin R.T. (2002) Formation of Ferrihydrite and Associated Iron Corrosion Products in Permeable Reactive Barriers of Zero-Valent Iron. *Environ. Sci. Technol.* **36,** 5469-5475.

Garcell L., Morales M.P., Andres-Verges M., Tartaj P., and Serna C.J. (1998) Interfacial and Rheological Characteristics of Maghemite Aqueous Suspensions. *J. Colloid Interface Sci.* **205,** 470-475.

He F. and Zhao D. (2005) Preparation and Characterization of a New Class of Starch-Stabilized Bimetallic Nanoparticles for Degradation of Chlorinated Hydrocarbons in Water. *Environ. Sci. Technol.* **39,** 3314-3320.

Ho Y.S. and McKay G. (1998) Pseudo-second order model for sorption processes. *Process Biochem.* **34,** 451-465.

Hwang Y., Kim D. and Shin H. (2015) Inhibition of nitrate reduction by NaCl adsorption on a nano-zero-valent iron surface during a concentrate treatment for water reuse. *Environ. Technol.* **36,** 1178-1187.

Kaplan D.I. and Hang T. (2007) Estimated Duration of the Subsurface Reduction Environment Produced by the Saltstone Disposal Facility on the Savannah River Site. *Washington Savannah River Company* WSRC-STI-2007-00046.

Kielemoes, J., De Boever, P. and Verstraete, W. (2000) Influence on Denitrification on the Corrosion of Iron and Stainless Steel Powder. *Environ. Sci. Technol.* **34,** 663-671.

Li H., Wan J., Ma Y., Huang M., Wang Y. and Chen Y. (2014) New insights into the role of zero-valent iron surface oxidation layers in persulfate oxidation of dibutyl phthalate solutions. *Chem. Eng. J.* **250,** 137-147.

Liu H., Qian T. and Zhao D. (2013) Reductive immobilization of perrhenate in soil and groundwater using starch-stabilized ZVI nanoparticles. *Chin. Sci. Bull.* **58,** 275-281.

Lenell B.A. and Arai Y. (2016) Evaluation of Perrhenate Spectrophotometric Methods in Bicarbonate and Nitrate Media. *Talanta.* **150,** 690-698.

Mallet M., Barthélémy K., Ruby C., Renard A. and Naille S. (2013) Investigation of phosphate adsorption onto ferrihydrite by X-ray Photoelectron Spectroscopy. *J. Colloid Interface Sci.* **407,** 95-101.

Moore A.M. and Young T.M. (2005) Chloride Interactions with Iron Surfaces: Implications for Perchlorate and Nitrate Remediation Using Permeable Reactive Barriers. *J. Environ. Eng.* **131,** 924-933.

Ponder S.M., Darab J.G., Mallouk T.E. (2000) Remediation of Cr(VI) and Pb(II) Aqueous Solutions Using Supported, Nanoscale Zero-valent Iron. *Environ. Sci. Technol.* **34,** 2564-2569.

Rennert T. and Mansfeldt T. (2002) Sorption of Iron-Cyanide Complexes on Goethite in the Presence of Sulfate and Desorption with Phosphate and Chloride **31,** 745-751.

Rodríguez-Maroto J.M., García-Herruzo F., García-Rubio A., Gómez-Lahoz C. and Vereda-Alonso C. (2009) Kinetics of the chemical reduction of nitrate by zero-valent iron.*Chemosphere* **74,** 804-809.

Roy A. (2009) Sulfur speciation in granulated blast furnace slag: An X-ray absorption spectroscopic investigation. *Cem. Concr. Res.* **39,** 659-663.

Saleh N., Sirk K., Liu Y., Phenrat T., Dufour B., Matyjazewski K., Tilton R.D. and Lowry G.V. (2007) Surface Modifications Enhance Nanoiron Transport and NAPL Targeting in Saturated Porous Media. *Environ. Eng. Sci.* **24,** 45-57.

Schulte E. and Scoppa P. (1987) Sources and Behavior of Technetium in the Environment. *Sci. Total Environ.* **64,** 163-179.

Schwochau K. (2000) *Technetium: chemistry and radiopharmaceutical applications*. Wiley-VCH, Weinheim.

Stucki J.W. (1981) The Quantitative Assay of Minerals for Fe^{2+} and Fe^{3+} Using 1,10-Phenanthroline: II A Photochemical Method. *Soil Sci. Soc. Am. J.* **45,** 638-641.

Sun Y., Li X., Cao J., Zhang W., and Wang H.P (2006) Characterization of zero-valent iron nanoparticles. *Adv. Colloid Interface Sci.* **120,** 47-56.

Suponik T., Winiarski A., Szade J (2015) Process of Removing Zinc from Water using Zero-Valent Iron. *Water Air Soil Pollut.* **226,** 360-371.

Tian H., Li J., Mu Z., Li L. and Hao Z. (2009) Effect of pH on DDT degradation in aqueous solution using bimetallic Ni/Fe nanoparticles. *Sep. Purif. Technol.* **66,** 84-89.

Van Bruwaene R., Hegela M., Gerber G. B., Kirchmann R. and Maisin J. R. (1986) Toxicity of Long-term Application of Dietary Technetium to Rats and their Offspring. In *Technetium in the Environment* (eds. G. Desmet and C. Myttenaere). Springer Netherlands, 391-396.

Xin J., Zheng X., Han J., Shao H., Kolditz O. (2015) Remediation of trichloroethylene by xanthan gum-coated microscale zero valent iron (XG-mZVI) in groundwater: Effects of geochemical constituents. *Chem. Eng. J.* **271,** 164-172.

Yang, G.C.C. and Lee H. (2005) Chemical reduction of nitrate by nanosized iron: kinetics and pathways. *Water. Res.* **39,** 884-894.

Yoon I., Bang S., Chang J., Kim M.G. and Kim K. (2011) Effects of pH and dissolved oxygen on Cr(VI) removal in Fe(0)/H_2O systems. *J. Hazard. Mater.* **186,** 855-862.

Yoshihara K. (1996) Technetium in the environment. In *Technetium and Rhenium Their Chemistry and Its Applications* (eds. K. Yoshihara and T. Omori). Springer Berlin Heidelberg.

Yuan P., Liu D., Fan M., Yang D., Zhu R., Ge F., Zhu J. and He H. (2010) Removal of hexavalent [Cr(VI)] from aqueous solutions by the diatomite-supported/unsupported magnetite nanoparticles. *J. Hazard. Mater.* **173,** 614-621.

Zhou J., Wang Y., Wang J., Qiao W., Long D. and Ling L. (2016) Effective removal of hexavalent chromium from aqueous solutions by adsorption on mesoporous carbon microspheres. *J. Colloid Interface Sci.* **462,** 200-207.

Chapter 4: Summary and Conclusion

Immobilization of radioactive waste products has become of increasing interest for the U.S. Department of Energy, specifically immobilization of pertechnetate (TcO_4^-). Pertechnetate is a low level radioactive waste that is highly mobile in a Tc(VII) oxidation state, whereas Tc(IV) compounds precipitate as insoluble solids, which are considerably less mobile. Cementitious waste technology (CWT) has been considered to immobilize $Tc(VII)O_4^-$, as Tc(IV) oxides and sulfides with the use of reducing agents like blast furnace slag, portland cement, and fly ash. The Savannah River Site has used a CWT formulation called 'saltstone', in order to immobilize hazardous wastes such as this. These types of treatment practices involve highly alkaline conditions, and high concentrations of anions, such as carbonate and nitrate. Zero valent iron (ZVI), has been considered as an additional reducing agent that could be used. In this study, the reduction capacity of ZVI for ReO_4^- , as a chemical surrogate for TcO_4^-, was evaluated in high carbonate solutions.

ReO_4^- can be immobilized in ZVI as much as 20% at pH 10.2 and 0.1M nitrate. Although overall immobilization was limited at high pH and high nitrate concentration, reduction of Re(VII) still had occurred. Over a broad pH range (4-12), most overall sorption had occurred under near neutral pH conditions. In low pH conditions, corrosion of the ZVI surface by H^+. Under high pH conditions, surface oxidation and Fe-oxyhydroxide layer formation likely passified the surface, lowering reaction effectiveness. A pseudo 2nd order sorption kinetic model was appropriate to fit the data. Rates increased with additions of nitrate. The reduction of nitrate produced NH_4^+ that neutralizes the surface charge of ZVI to facilitating the electron transfer reaction. Considering the thermodynamically favorable reduction of Tc(VII) over Re(VII), ZVI have potential for improving the current CWT. This study provides insight towards a new cement formulation with ZVI to immobilization of TcO_4^- in low level radioactive waste streams.